Probing eV-Scale Axions with the CAST experiment at CERN

Julia Vogel

Albert-Ludwigs-Universität Freiburg,Germany

Seminar in Louvain-la-Neuve

November 26, 2009

CAST

The CAST Experiment

Canada
University of British Columbia, Vancouver
M. Hasinoff

Croatia
Rudjer Bošković Institute, Zagreb
K. Jakovčić, M. Krčmar, B. Lakić, A. Ljubičić

France
DAFNIA, CEA-Saclay, Gif-sur-Yvette
S. Aune, T. Dafni, E. Ferrer-Ribas, I. Giomataris, T. Papaevangelou

Germany
Albert-Ludwigs-Universität Freiburg
H. Fischer, J. Franz, D. Kang, E. Gruber, T. Guthörl, K. Königsmann, J. Vogel

TU Darmstadt, Institut für Kernphysik
H. H. Hoffmann, M. Kuster, A. Nordt, H. Riege

Universität Frankfurt
J. Jacoby

MPE Garching
H. Bräuninger, R. Hartmann, P. Friedrich, M. Kuster, A. Nordt

MPI München
R. Kotthaus, G. Lutz, A. Mirrizi, G. Raffelt

MPI für Sonnensystemforschung, Katlenburg-Lindau
S. Solanki

Greece
University of Patras
Y. Semertzidis, M. Tsagri, K. Zioutas

National Center for Scientific Research „Demokritos“, Athen
G. Fanourakis, T. Geralis, K. Kousouris

Aristotle University of Thessaloniki
C. Eleftheriadis, A. Liolios, I. Savvidis, T. Vafeiadis

National Technical University of Athens, Athen
E. Gazis, T. Karageorgopoulus

Italy
INFN Trieste
G. Cantatore, M. Karuza, V. Lozza, G. Raiteri

Russia
Russian Academy of Science, Moskow
A. Belov, S. Gninenko

Switzerland
CERN, Genf
K. Barth, S. Borghi, M. Davenport, F. Haug, L. Di Lella, N. Elias, C. Lasseur, H. Mota, T. Niinikoski, A. Palacci, H. Riege, P. Serpico, P. S. Silva, L. Stewart, L. Walckiers, Y. Wong

Spain
University of Zaragoza
J. Carmona, S. Cebrián, J. Galán, H. Gómez, F. J. Iguaz, I. G. Irastorza, G. Luzón, J. Morales, A. Ortiz, A. Rodriguez, J. Ruz, J. Villar

Turkey
Dogus University, Istanbul
S. Boydag, S. A. Cetin, C. Ezer, I. Hikmet

USA
Lawrence Livermore National Laboratory
M.Pivovaroff, R. Soufli, K. van Bibber

University of Chicago, Enrico Fermi Institute and KICP
J. Collar, D. Miller

Overview

1. Theoretical motivation for axions
2. Search for solar axions with helioscopes
3. The CAST-Experiment
4. X-ray mirror optics and CCD detector
5. Exemplary Analysis of the ^{4}He data
6. Results and Prospects

Theoretical Motivation for Axions

Theoretical Motivation for Axions

The strong CP-problem

CP-violation necessary in the standard model:
Explanation of matter-antimatter-asymmetry

CP-violation in weak interactions
CP-conservation in electromagnetic+strong interactions

QCD predicts violation in strong interactions

$$L_\theta = \bar{\theta} \frac{g^2}{32\pi^2} G^a_{\mu\nu} \tilde{G}^{\mu\nu}_a \quad \text{mit} \quad \tilde{G}^{\mu\nu}_a = -\frac{1}{2} \varepsilon^{\mu\nu\alpha\beta} G^a_{\alpha\beta}$$

HOWEVER:

So far no experiment has observed this CP-violation in QCD!

Theoretical Motivation for Axions

The Peccei-Quinn-Solution

A possible solution to the strong CP-problem:

Elimination of CP-violating term in QCD Lagrangian by introduction of new additional global U(1) symmetry

$$L_a = C \frac{a}{f_a} \frac{g^2}{32\pi^2} G^a_{\mu\nu} \tilde{G}^{\mu\nu}_a$$

→ New pseudo-scalar field → **AXION**

→ First proposed by Peccei & Quinn (1977)

→ Particle interpretation by Weinberg, Wilczek (1978)

The Axion: Properties

- Neutral pseudo-scalar Goldstone-Boson
- Only feable interaction with ordinary matter
- Mass (from axion-π^0-mixing): $$m_a \approx 0.6\,\text{eV}\,\frac{10^7\,\text{GeV}}{f_a}$$ $$f_a > 10^7\,\text{GeV} \qquad \text{(Astrophysical criterion)}$$
- Coupling to photons: $$L_{a\gamma} \approx g_{a\gamma}\left(\vec{E}\cdot\vec{B}\right) a \quad \text{with} \quad g_{a\gamma} \approx \frac{\alpha}{2\pi f_a} < 10^{-10}\,\text{GeV}^{-1}$$
- Mean lifetime: $$\tau_a \approx 10^{17}\,\text{yr} \quad \text{for} \quad m_a = 1\,\text{eV} \quad \text{i.e.} \quad \tau_a > t_{\text{Universe}}$$

The Axion: Models

Distinguishing feature for different axion models is size of PQ breaking scale:

$$f_a \propto \frac{1}{m_a}$$

- **„Visible Axion“ (PQWW-Axion)**
  - → Large axion mass ($m_a \gtrsim$ **150 keV**), since $f_a \approx f_{weak} \approx 250\,\mathrm{GeV}$
  - → Excluded by experiments and theory
- **„Invisible Axion“**
  - → Small axion mass ($m_a \approx$ **µeV-eV**)
  - → **K**im-**S**hifman-**V**ainshtein-**Z**akharov-Model
    Exotic, heavy quark carries PQ-charge
  - → **D**ine-**F**ischler-**S**rednicki-**Z**hitnitskii-Model
    SM fermions carry PQ-charge

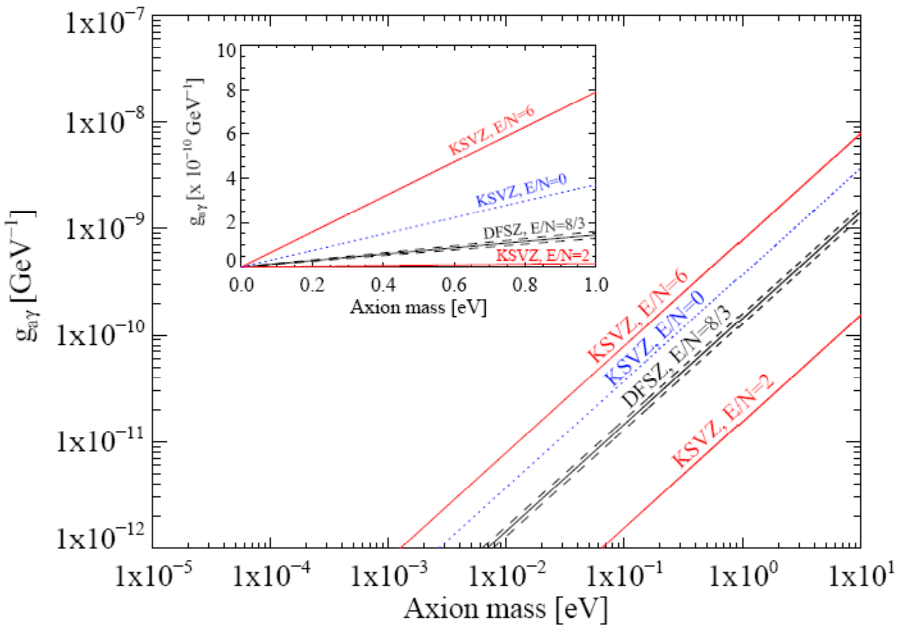

The Axion: Killing two birds with one stone

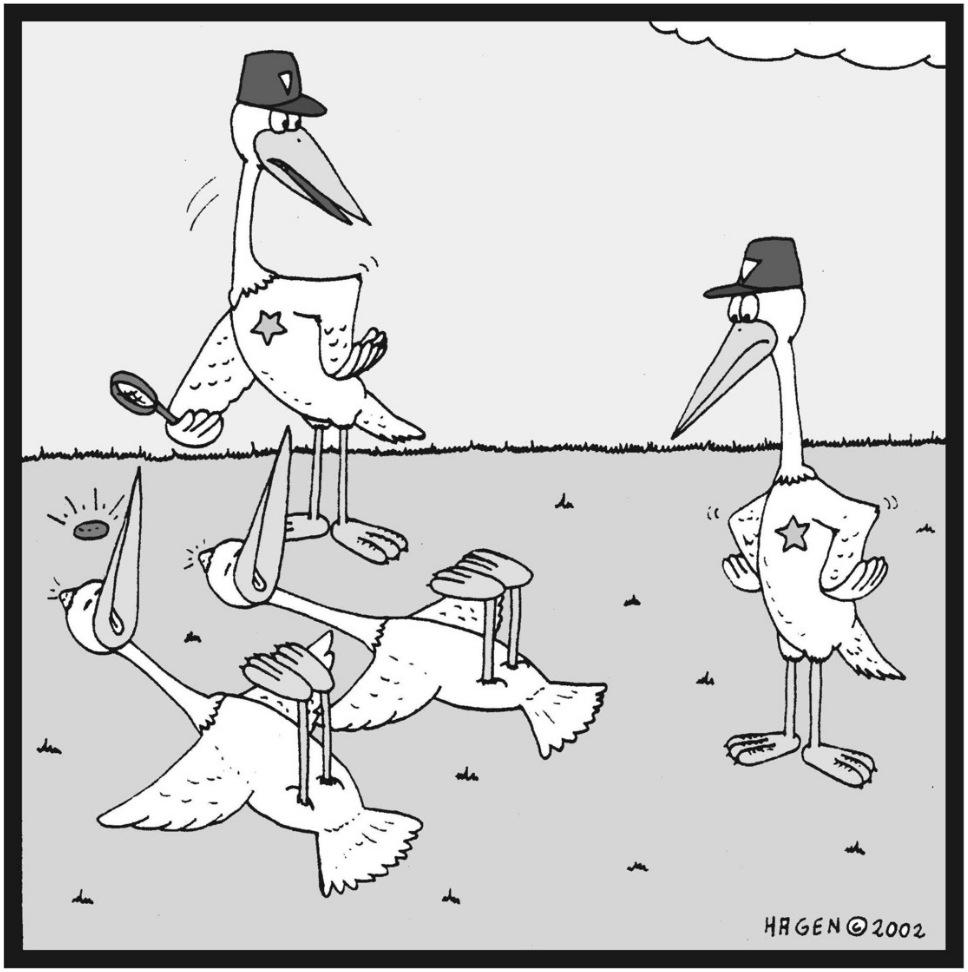

Unbelievable! It looks like they've
both been killed by the same stone...

Axions as

→ **Solution to the strong CP-problem**

→ **Candidate for dark matter**

Theoretical Motivation for Axions

The Axion: Experimental searches

- **Galactic axions**
  - → Haloscopes (ADMX, Carrack)
  - → Telescopes (Haystack)
- **Laboratory axions**
  - → Shining-Light-through-Walls (OSQAR, LIPSS, ALPS)
  - → Polarization (PVLAS)
- **Solar axions**
  - → Crystals (SOLAX,COSME)
  - → Helioscopes (Tokyo, **CAST**)

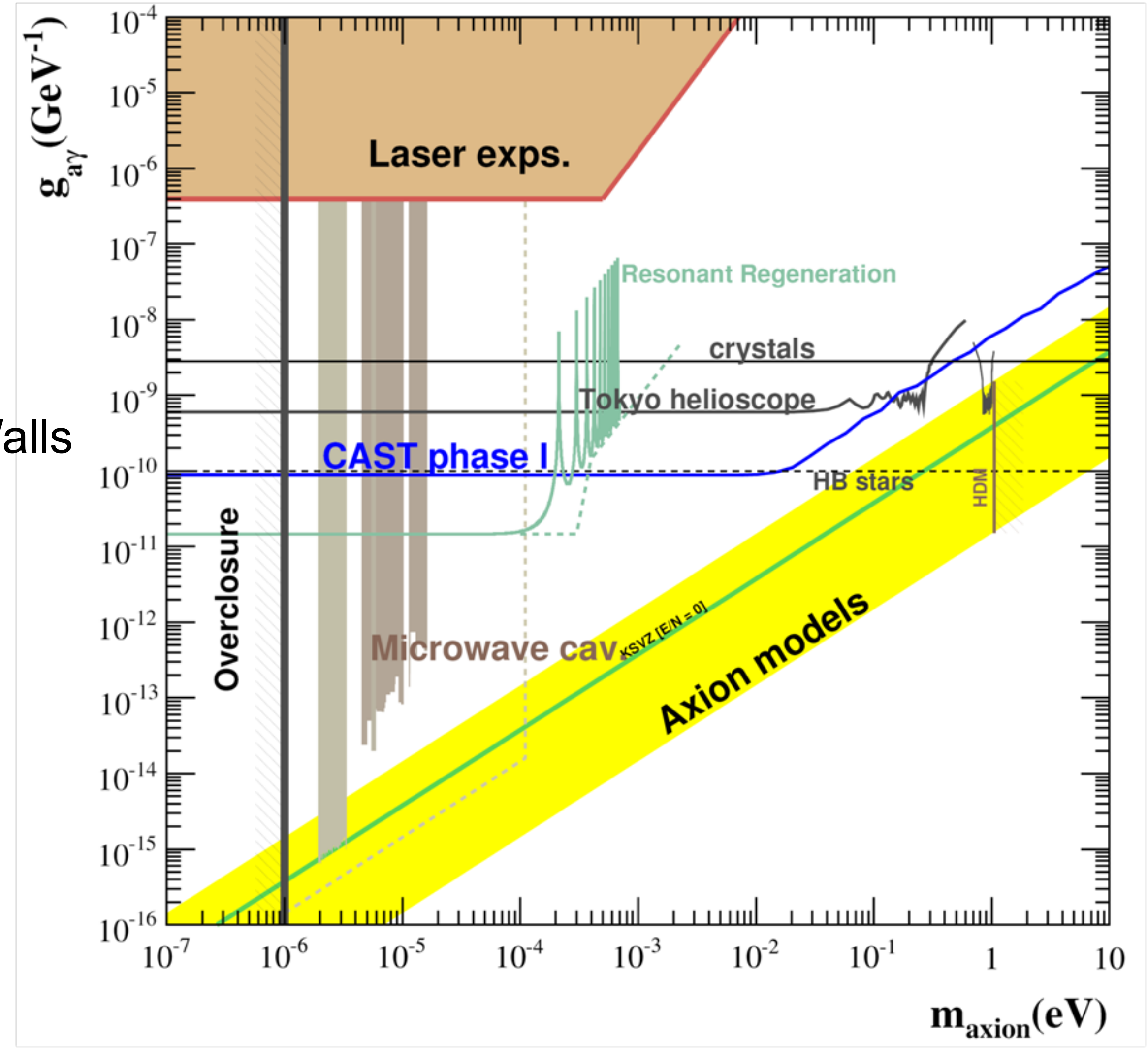

Search for solar axions with helioscopes

Primakoff-Effect:

Photons of blackbody radiation (X-ray photons) —— Strong electric fields in solar core ——→ Axions

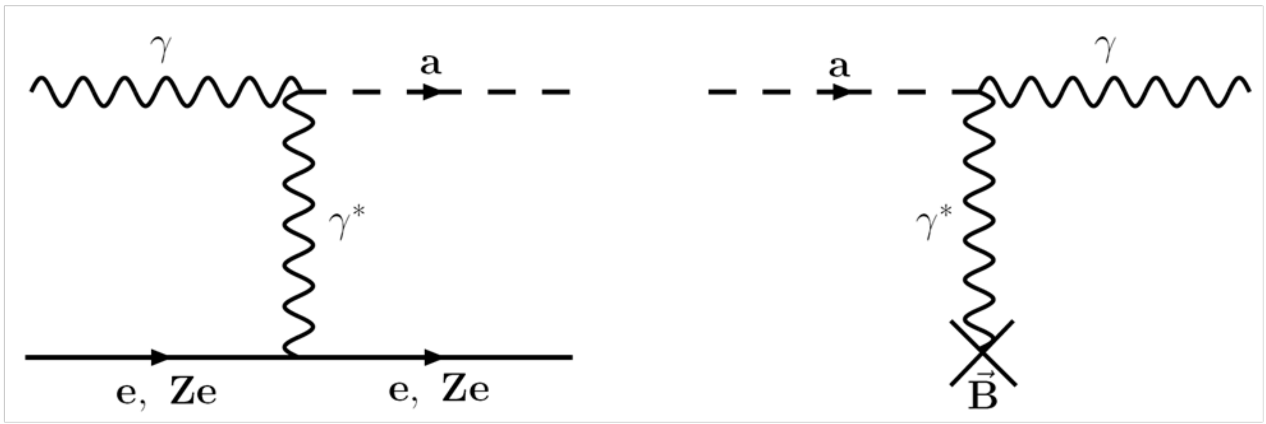

Inverse Primakoff-Effect:

Axions —— Strong magnetic field in laboratory on Earth ——→ X-ray photons

Production and detection of axions

Primakoff-Effect:

Photons of blackbody radiation (X-ray photons) —— Strong electric fields in solar core ——> Axions

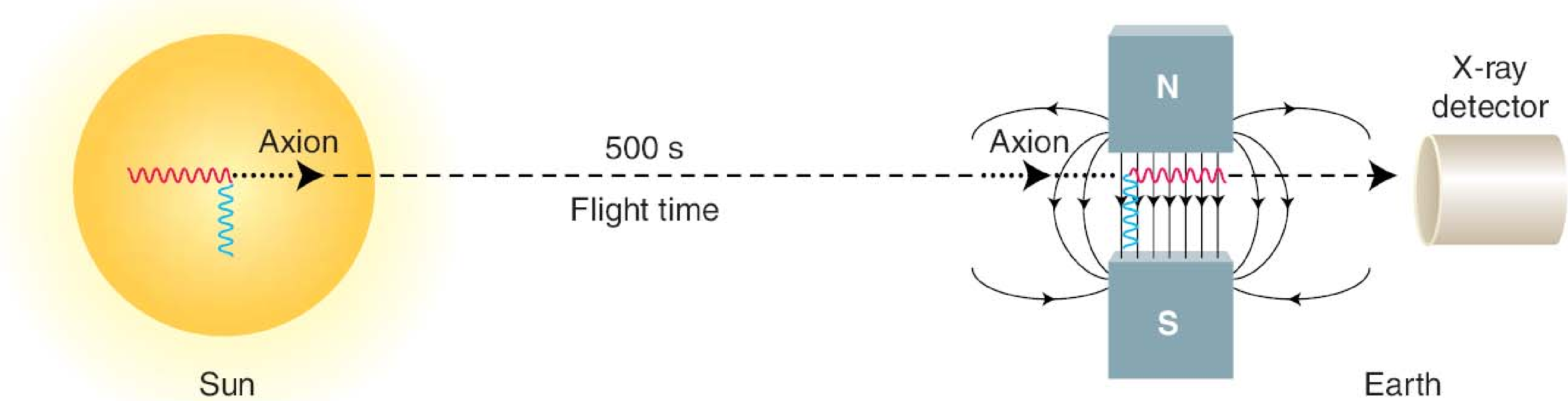

Inverse Primakoff-Effect:

Axions —— Strong magnetic field in laboratory on Earth ——> X-ray photons

Expected solar axion flux at Earth

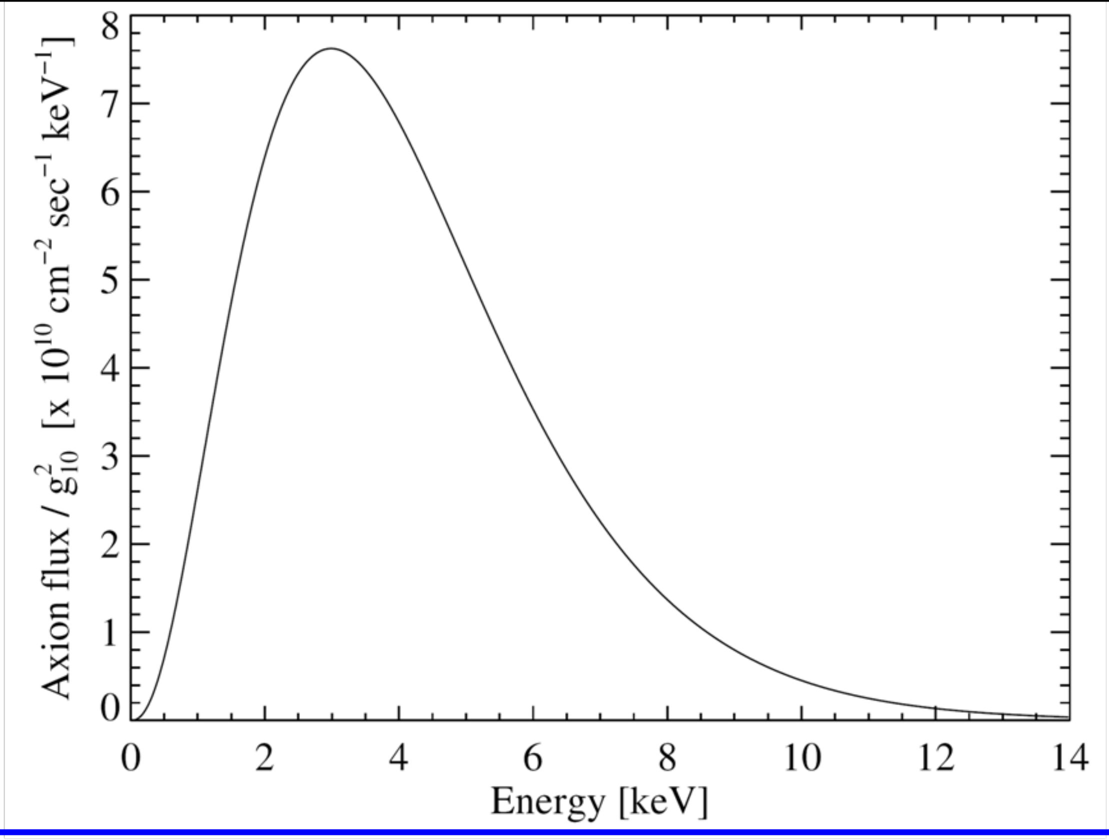

- Mean Energy of axions: $\langle E_a \rangle = 4.2$ keV
- Flux of axions: $$\frac{d\Phi_a(E_a)}{dE_a} \propto g_{a\gamma}^2 \frac{E_a^{2.481}}{e^{E_a/1.205}}$$

(Serpico & Raffelt, based on standard solar model BP2004 of Bahcall et al.)

Conversion probability and coherence condition

$$P_{a\to\gamma} = \left(\frac{Bg_{a\gamma}}{2}\right)^2 \frac{1}{q^2 + \Gamma^2/4}\left[1 + e^{-\Gamma L} - 2e^{-\Gamma L/2}\cos(qL)\right]$$

With momentum transfer $q = \left|\frac{m_\gamma^2 - m_a^2}{2E_a}\right|$, effective photon mass $m_\gamma[eV] \approx \sqrt{0.02\frac{P[mbar]}{T[K]}}$ in ^4He and absorption Γ

Conversion probability and coherence condition

$$P_{a\to\gamma} = \left(\frac{Bg_{a\gamma}}{2}\right)^2 \frac{1}{q^2 + \Gamma^2/4}\left[1 + e^{-\Gamma L} - 2e^{-\Gamma L/2}\cos(qL)\right]$$

With momentum transfer $q = \left|\frac{m_\gamma^2 - m_a^2}{2E_a}\right|$, effective photon mass $m_\gamma[eV] \approx \sqrt{0.02\frac{P[mbar]}{T[K]}}$ in ^{4}He and absorption Γ

$$P_{a\to\gamma} = \left(\frac{BLg_{a\gamma}}{2}\right)^2 \frac{\sin^2\left(qL/2\right)}{\left(qL/2\right)^2}$$

(if absorption Γ = 0)

Conversion probability and coherence condition

$$P_{a\to\gamma} = \left(\frac{BLg_{a\gamma}}{2}\right)^2 \frac{\sin^2\left(\frac{qL}{2}\right)}{\left(\frac{qL}{2}\right)^2}$$

(if absorption Γ = 0)

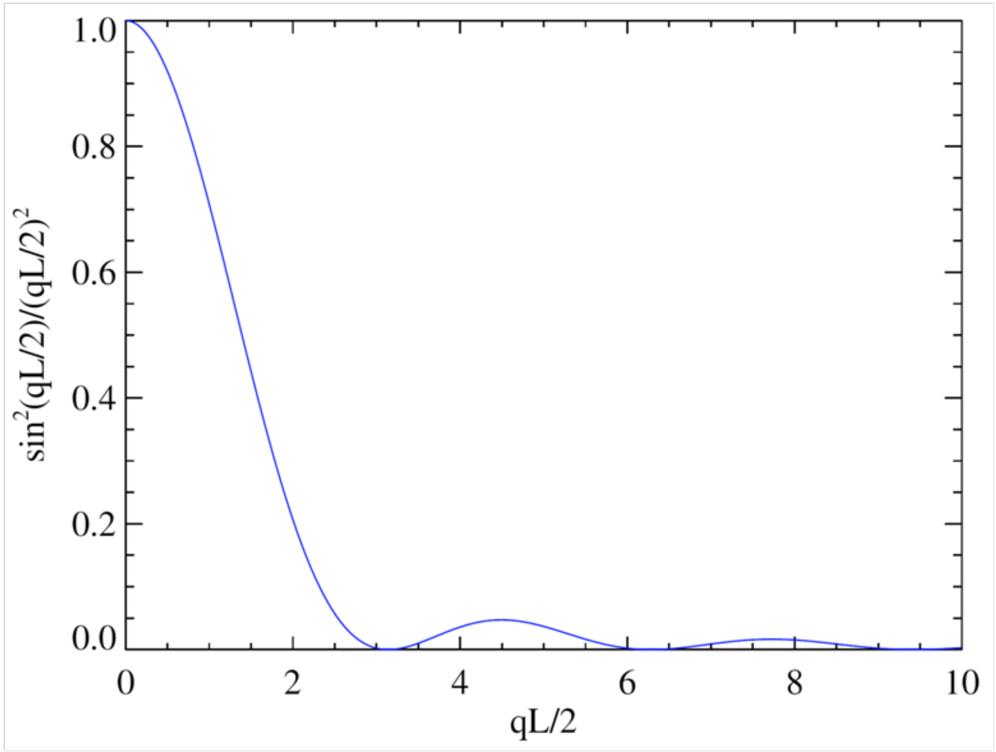

➡ Coherence condition:

$qL/2 < \pi$

Conversion probability and coherence condition

Coherence condition: $qL/2 < \pi$

CAST Phase I:
Vacuum in magnet
($m_\gamma = 0$, $qL/2 < \pi$)

Effective mass of photon $m_\gamma = 0$

$$q = \left|\frac{m_\gamma^2 - m_a^2}{2E_a}\right| = \frac{m_a^2}{2E_a}$$

Range of axion masses: $m_a \leq 0.02$ eV

CAST Phase II:
^4He / ^3He in magnet
($m_\gamma \neq 0$, $qL/2 < \pi$)

Effective mass of photon $m_\gamma > 0$

$$m_\gamma[eV] \approx \sqrt{0.02 \frac{P[mbar]}{T[K]}}$$

Extended range of axion masses
0.02 eV < m_a < 1.16 eV

Search for solar axions with helioscopes

Expected number of photons from axion conversion

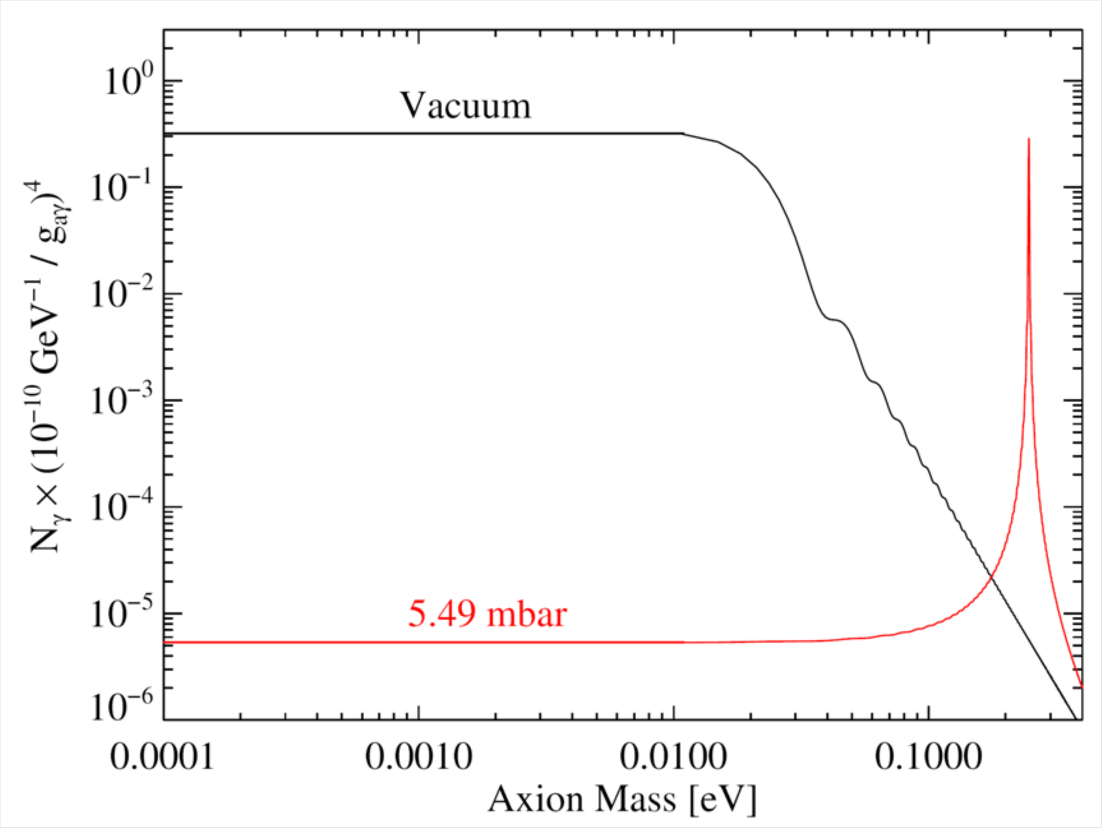

$$N_\gamma = \int \frac{d\Phi(E_a)}{dE_a} P_{a\to\gamma}(E_a)\, A\, \Delta t\, \varepsilon(E_a)\, dE_a \propto g_{a\gamma}^4$$

A: detector area, Δt: exposure time, $\varepsilon(E_a)$: efficiency

The CAST-Experiment

The CAST Experiment

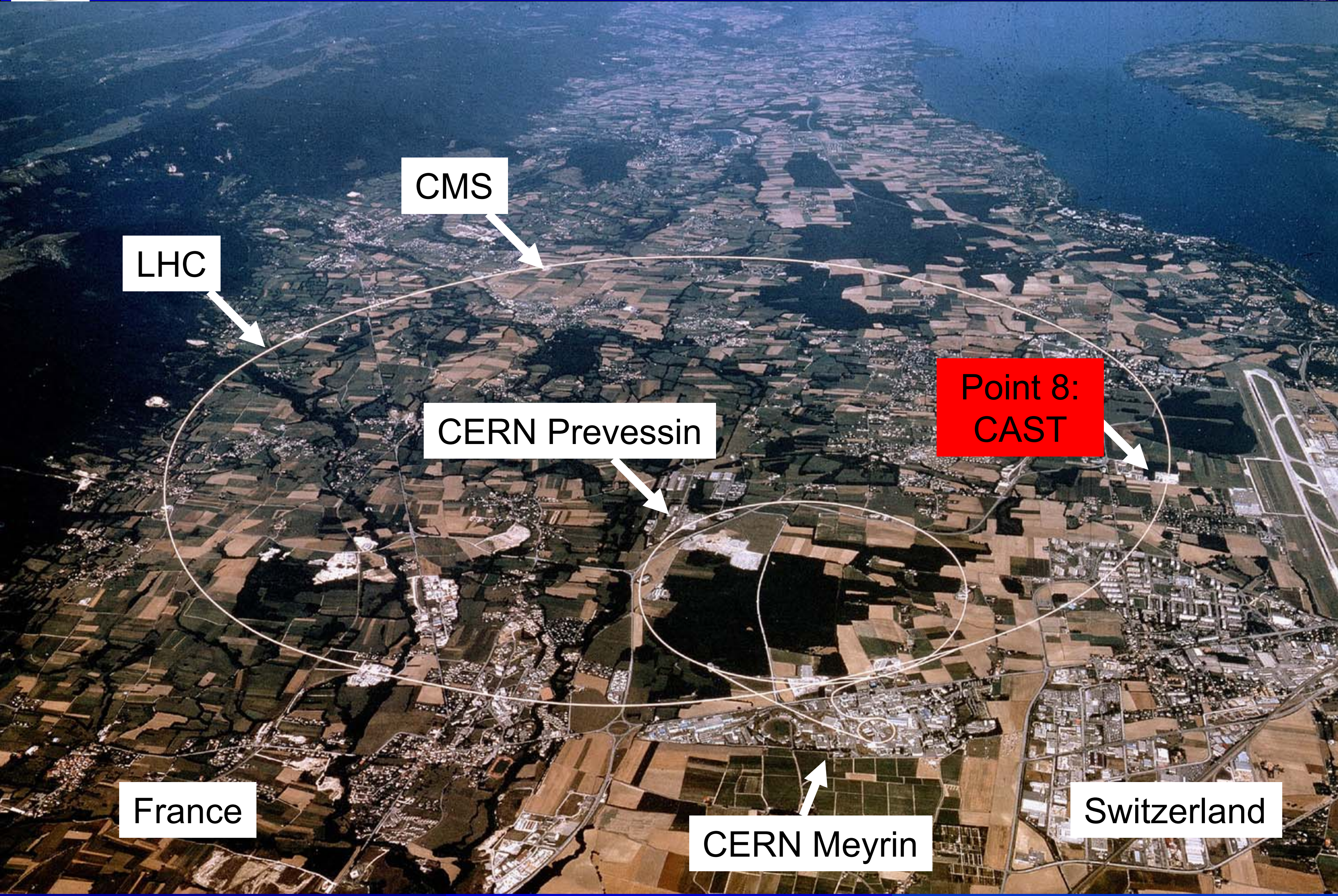

Experimental Setup

- Prototype of an LHC dipole magnet (B=9.0 Tesla, L=9.3 m, T=1.8 K)
- Range of movement: 80° horizontally and ± 8° vertically
- Solar tracking possible during sunrise and sunset (2 x 1.5 h per day)
- Three X-ray detectors and one X-ray mirror optics:
  MicroMEGAS (MM), Charge Coupled Device (CCD),Time Projection Chamber (TPC)

Experimental Setup

- Prototype of an LHC dipole magnet (B=9.0 Tesla, L=9.3 m, T=1.8 K)
- Range of movement: 80° horizontally and ± 8° vertically
- Solar tracking possible during sunrise and sunset (2 x 1.5 h per day)
- Three X-ray detectors and one X-ray mirror optics:
  MicroMEGAS (MM), Charge Coupled Device (CCD),MicroMEGAS (MM)

The CAST Experiment

Solar Filming

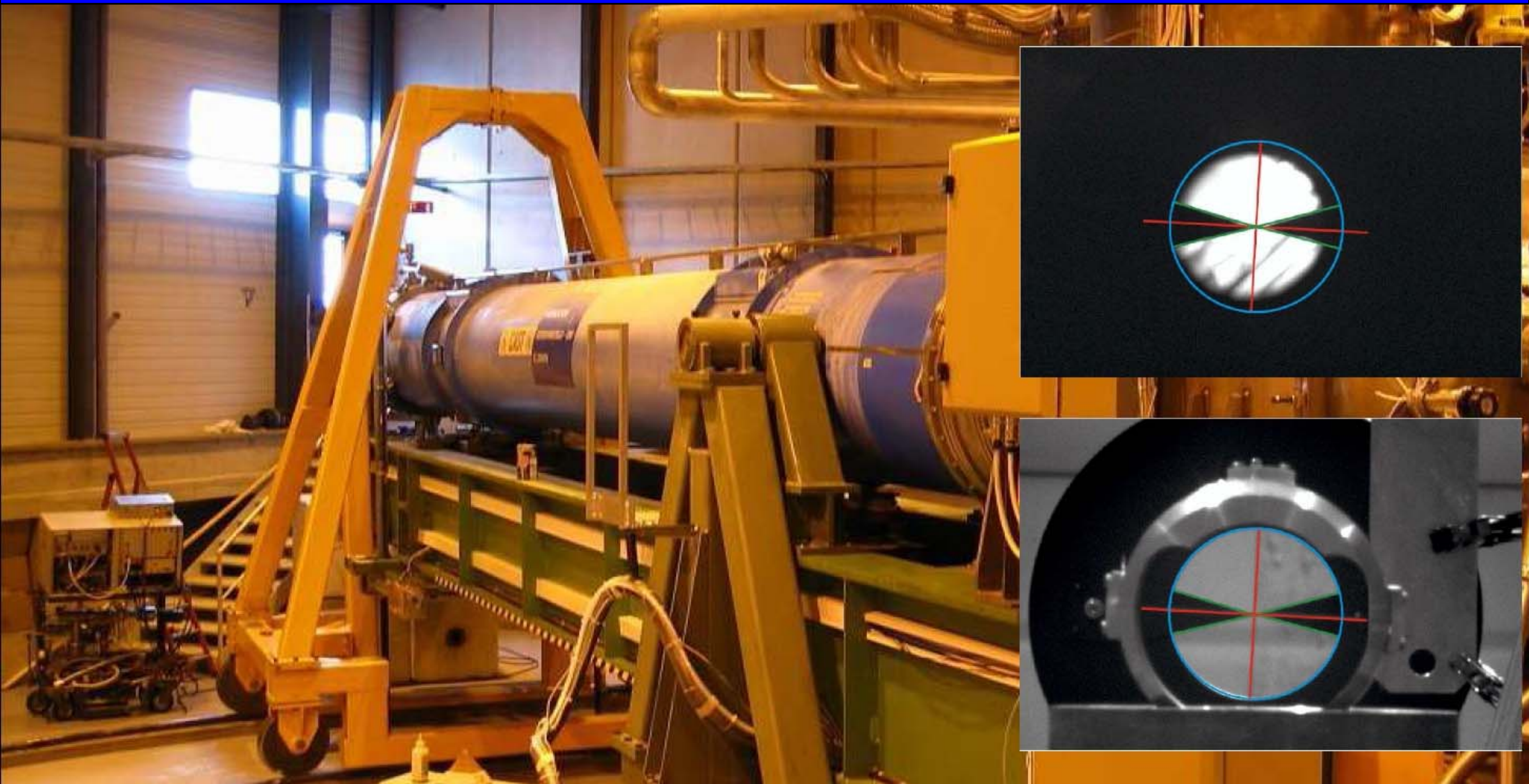

In March and September, Sun is directly observable through window:
CAST is able to follow the Sun with required accuracy (0.02°)!

The CAST Experiment

Vacuum and helium gas system

Phase I : Vacuum (2003+2004)

Phase II: ^4He (2005+2006)

^3He (2007- 2010)

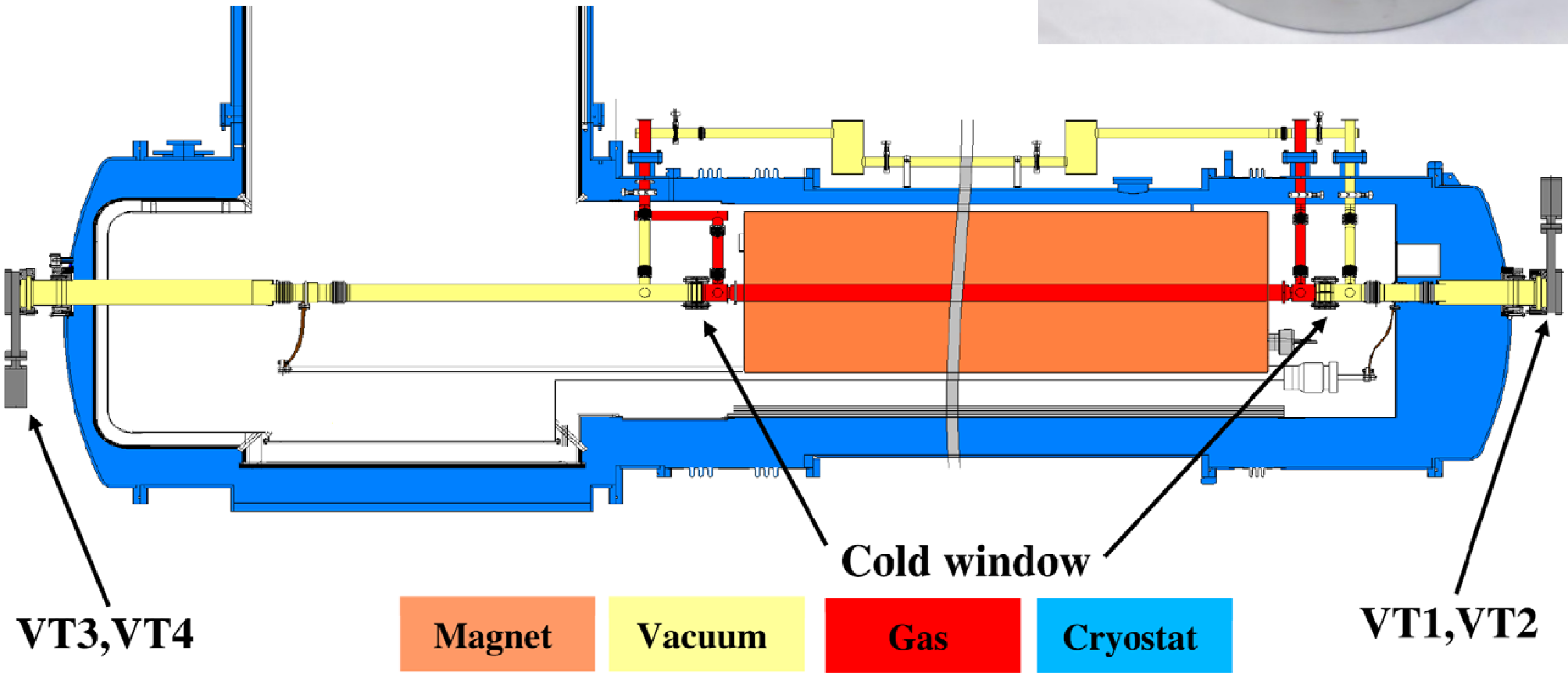

CAST detectors until 2006 (Phase I and II with ^4He)

MicroMEGAS

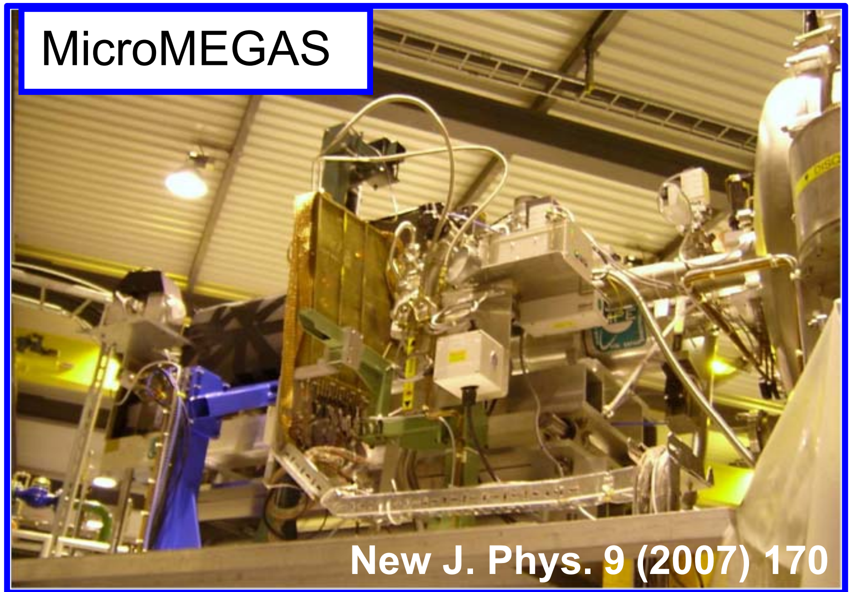

New J. Phys. 9 (2007) 170

X-ray telescope with CCD

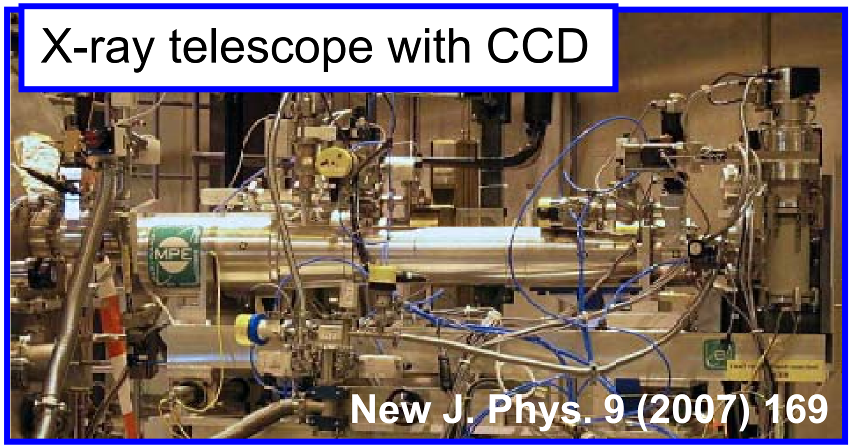

New J. Phys. 9 (2007) 169

Background count rates:

TPC:	85	cts/h (2-12 keV)
MM :	25	cts/h (2-10 keV)
Telescope/CCD:	0.25	cts/h (1- 7 keV)

TPC

New J. Phys. 9 (2007) 171

Sunrise detectors

Sunset detector

The CAST Experiment

Detector upgrades since 2007 (Phase II with ^{3}He)

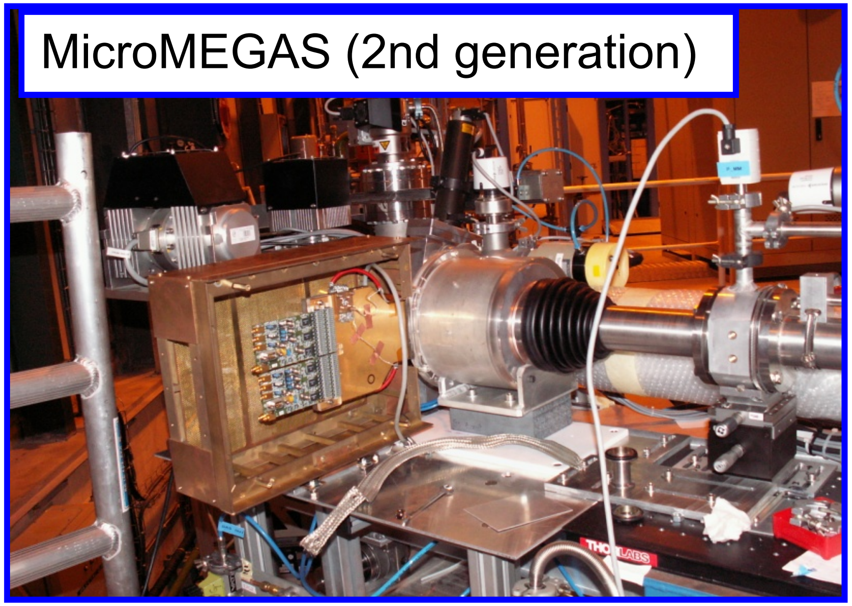

MicroMEGAS (2nd generation)

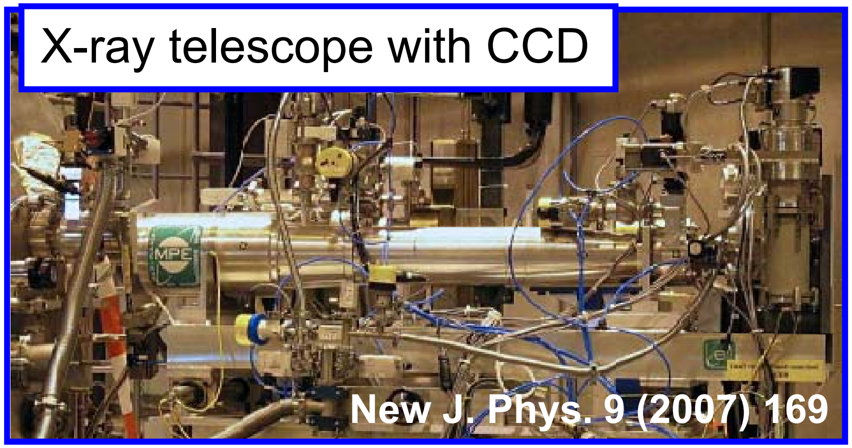

X-ray telescope with CCD

Background count rates:

MM : 3 cts/h (2-10 keV)

Teleskope/CCD: 0.16 cts/h (1- 7 keV)

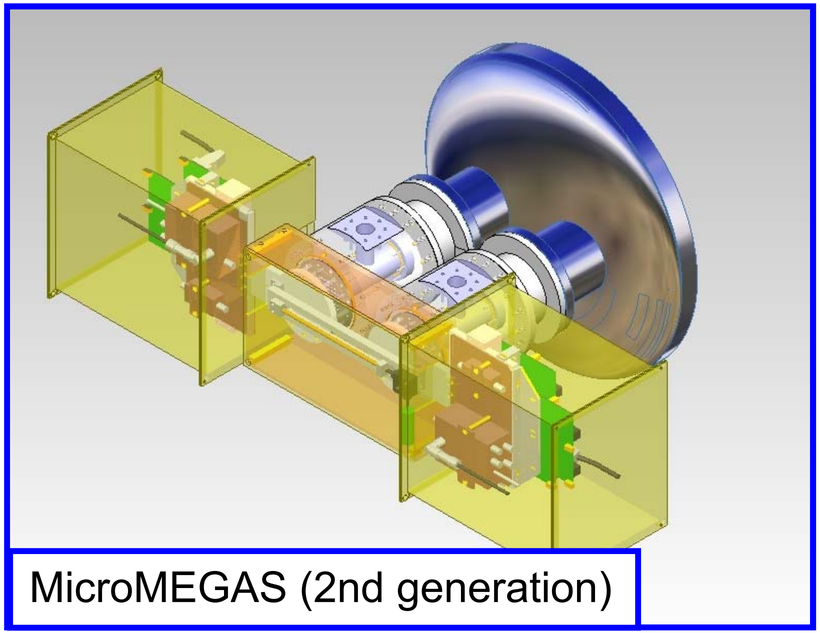

MicroMEGAS (2nd generation)

Sunrise detectors

Sunset detectors

The CAST Experiment

Detector upgrades since 2007 (Phase II with ^{3}He)

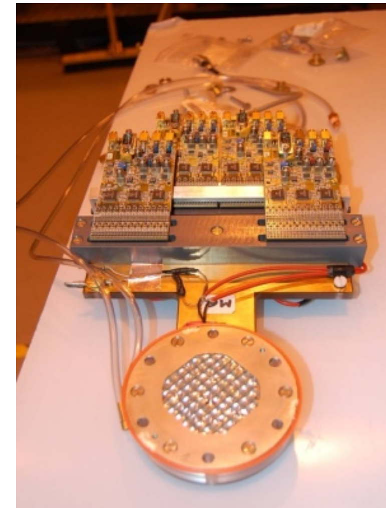

2nd generation Micromegas:

- Novel manufacturing technique (microbulk technology)
- Materials selected based on low intrinsic radioactivity
- Improved shielding

→ Good potential for very-low background rates

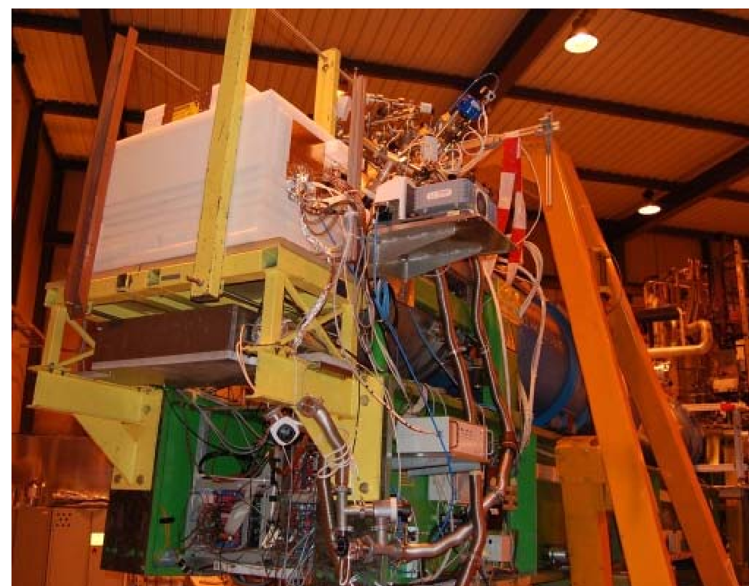

X-Ray Mirror Optics
and
CCD Detector

X-ray mirror optics and CCD detector

Experimental Setup

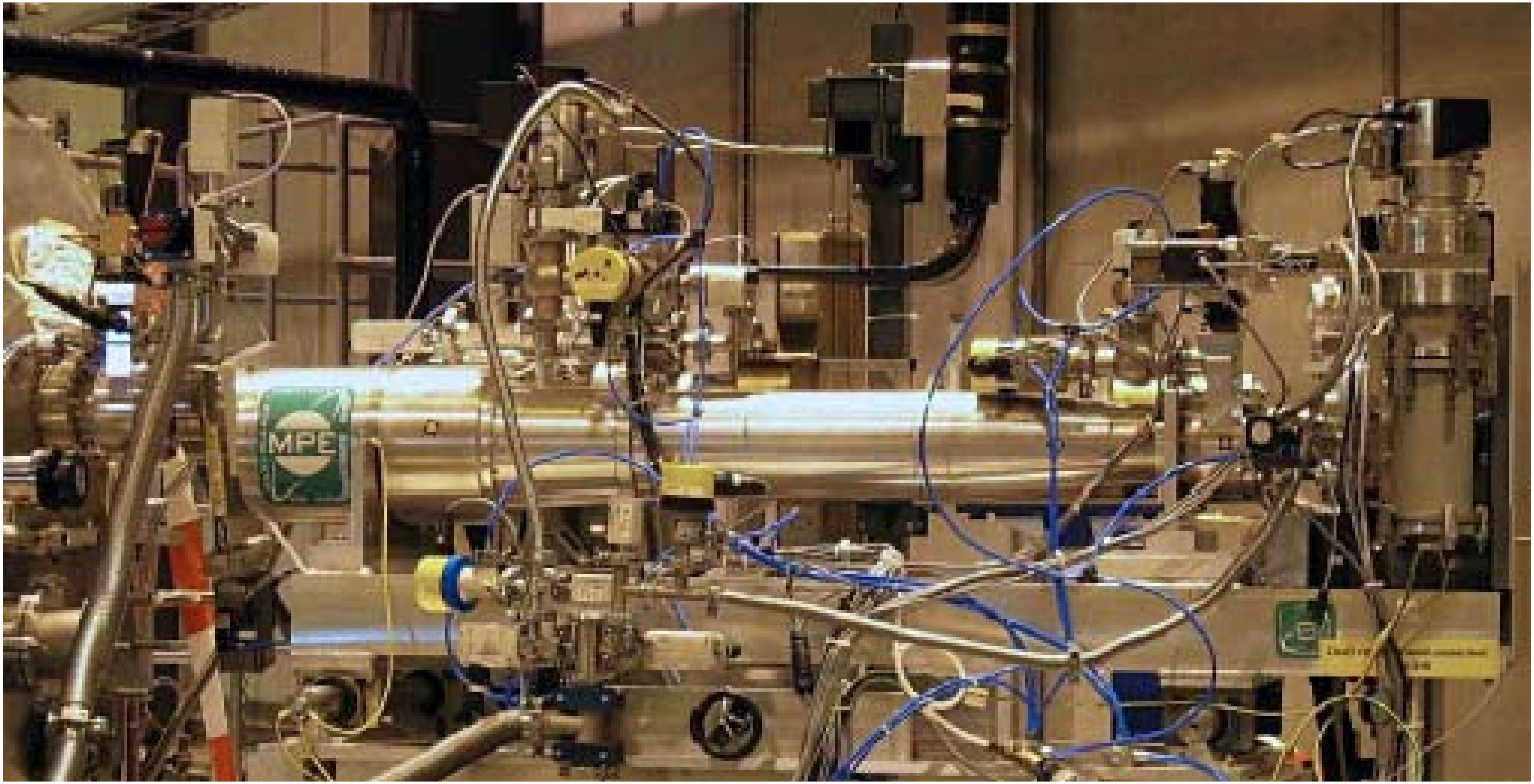

X-ray mirror optics and CCD detector

Experimental Setup

- Wolter-I-type telescope (Prototype of ABRIXAS mission)
- 27 nested, gold-coated mirror shells
- Only one sector of telescope illuminated at CAST

- pn-CCD (Prototype of XMM-Newton mission)
- Very good spatial and energy resolution
- Simultaneous measurement of signal and background possible

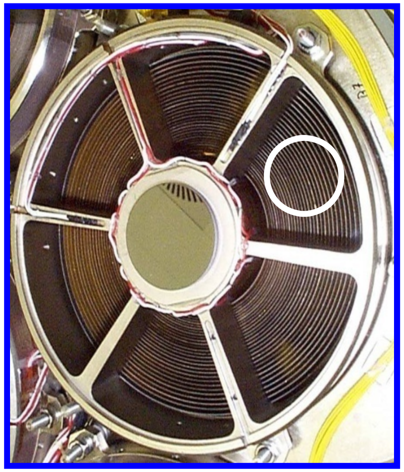

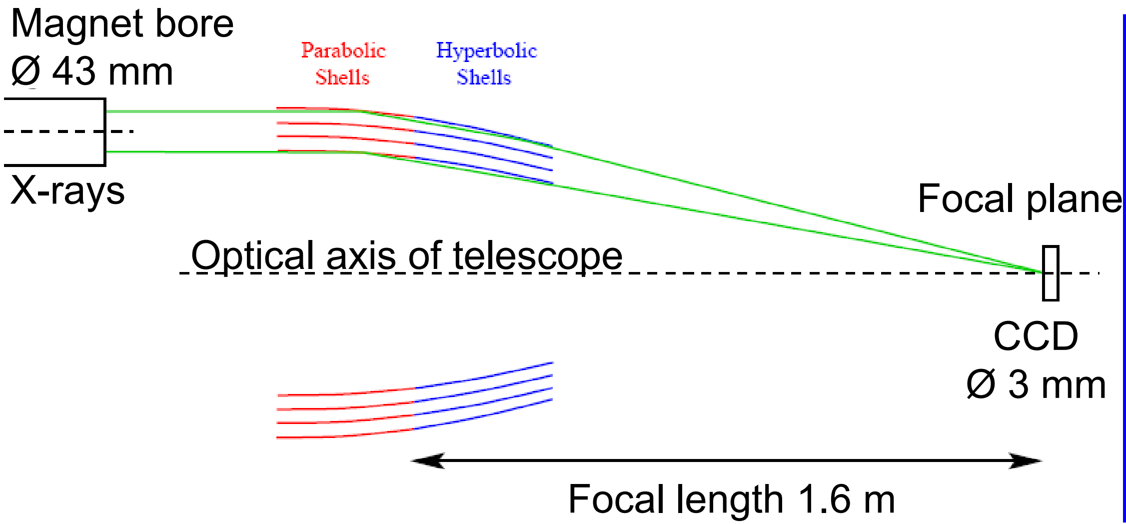

➡ Improvement of signal-to-background ratio by a factor of ~150!

Characterization of X-ray telescope (Optics + CCD)

Efficiency for X-ray mirror optics and CCD detector for CAST Phase I und II (^{4}He)

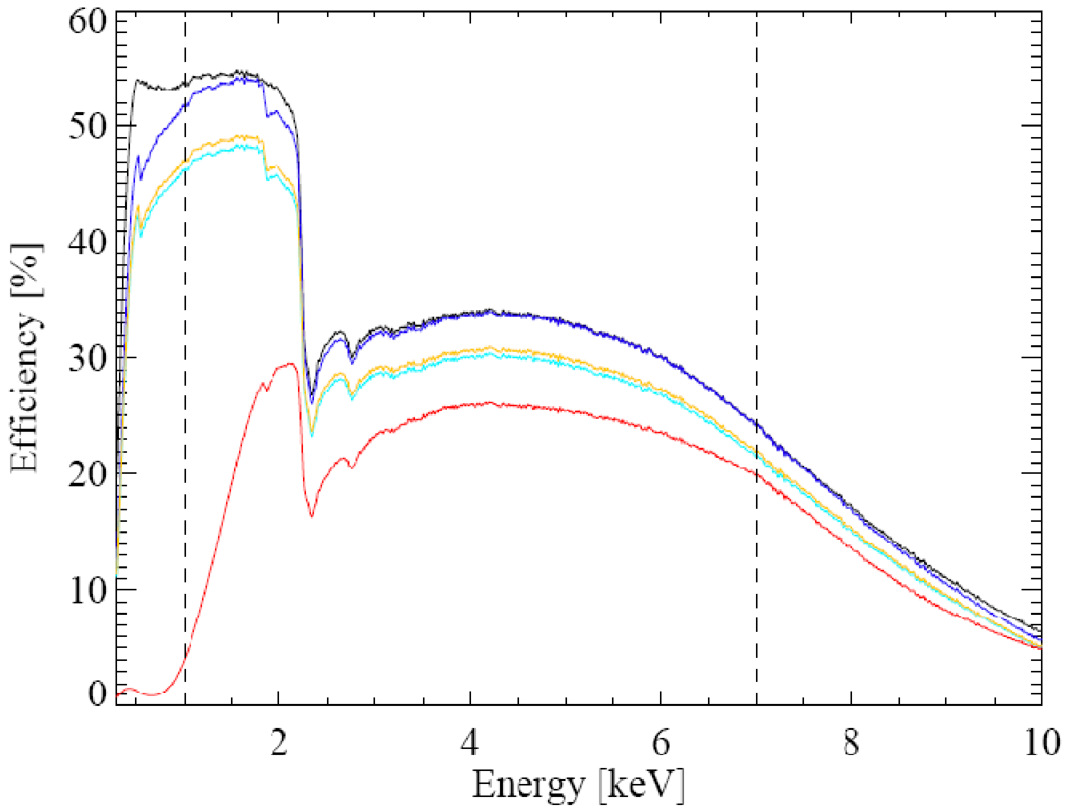

- **X-ray mirror optics for CAST**
- **Mirror optics + QE of CCD (Phase I)**
- **Consideration of the Cold Window (Phase II, from 2005 on)**

X-ray mirror optics and CCD detector

In-situ calibration of detector

X-Ray Tube – Ti-K Lines

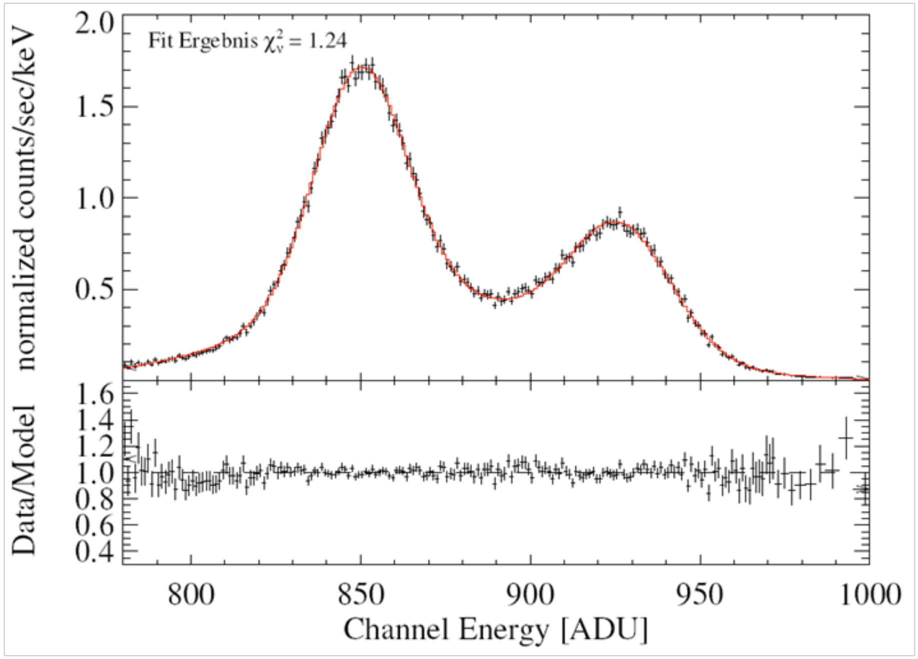

Background

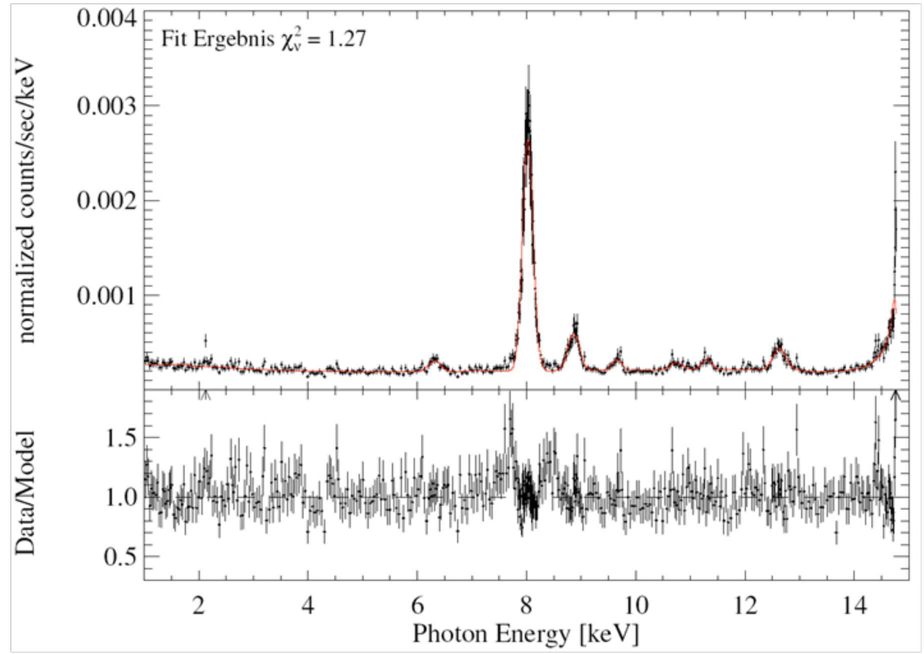

- Calibration of detector at CAST using X-ray tube
- Lines in background spectrum used for E > 10 keV
- Detector is calibrated till about 14 keV: absolute energy calibration better than 1%
- Additionally daily calibrations with ^{55}Fe (Energy resolution: 170 eV @ 5.9 keV)

X-ray mirror optics and CCD detector

Experimental background

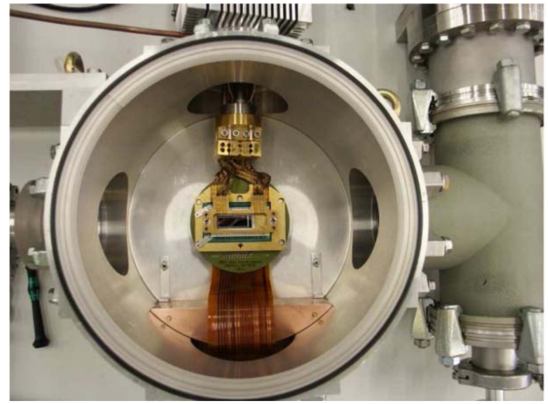

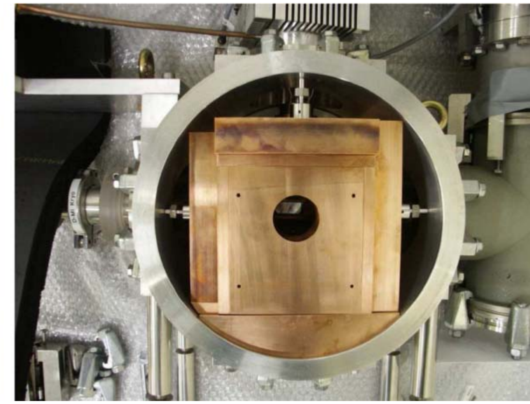

Rare event search:

→ Reduction of background

→ Material close to detector

- Pattern recognition algorithm
  - → MIP´s
- Shielding
  - → Inner part:
    1-4 cm Cu & 2.2 cm Pb
    External γ-Background
  - → Outer part:
    Pb against γ's (walls)
- Focussing via telescope
  - → Minimization of
    detector volume

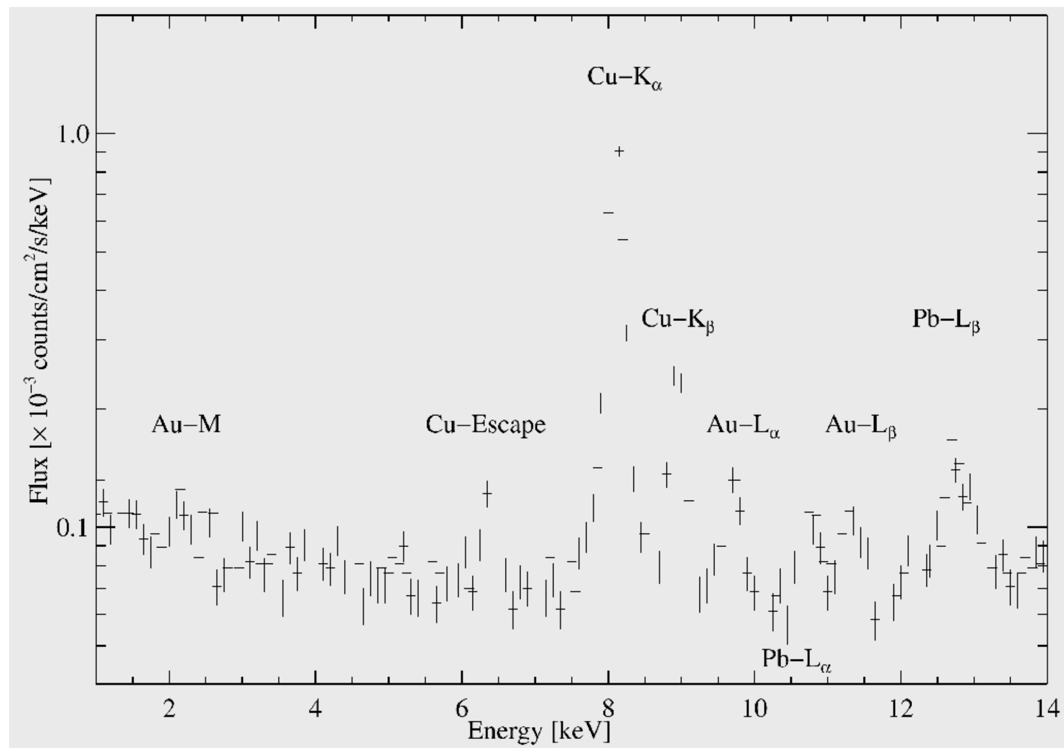

Upgrade CCD Frame-Store Detector

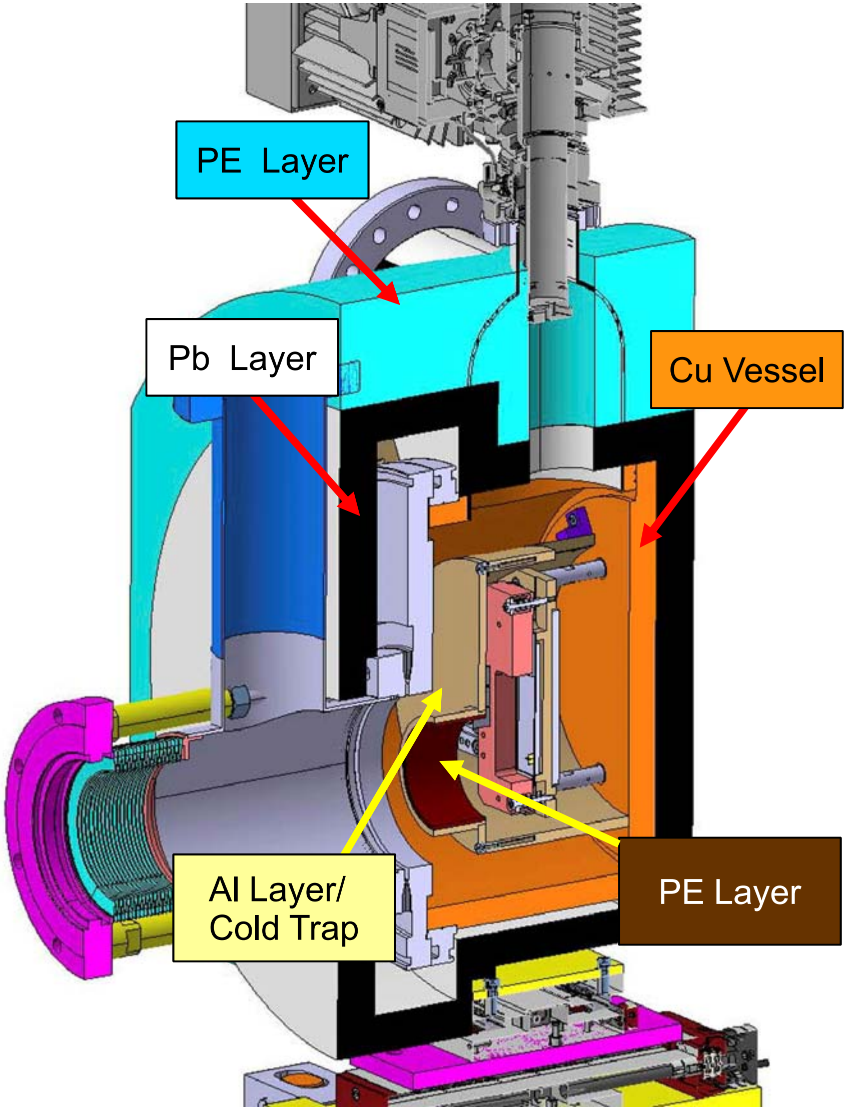

Frame-Store CCD Design

- Better low energy response
  - → 0.2 keV < E < 1keV
- Use of radiopure material+shielding
  - → Lower background
- Less out of time events
  - → 8% of measured flux
- State of the art technology
  - → Supported by other laboratories
- Decoupling of telescope and detector
  - → Simplification of alignment

Exemplary Analysis of the ^{4}He data

Expected signal for the CCD detector

For one helium density setting P_k one expects $N_{\gamma,k}$ photons from axion-to-photon conversion via Primakoff-effect:

$$N_{\gamma,k} = N_\gamma(P_k, m_a, g_{a\gamma}^4) = \int \frac{d\Phi(E_a, g_{a\gamma}^2)}{dE_a} P_{a\to\gamma,k}(E_a, m_a, g_{a\gamma}^2)\, \varepsilon(E_a)\, \Delta t_k\, A\, dE_a$$

Expected signal: Efficiency and axion flux

For one helium density setting P_k one expects $N_{\gamma,k}$ photons from axion-to-photon conversion via Primakoff-effect:

$$N_{\gamma,k} = N_\gamma(P_k, m_a, g_{a\gamma}^4) = \int \frac{d\Phi(E_a, g_{a\gamma}^2)}{dE_a} P_{a\to\gamma,k}(E_a, m_a, g_{a\gamma}^2)\,\varepsilon(E_a)\,\Delta t_k\, A\, dE_a$$

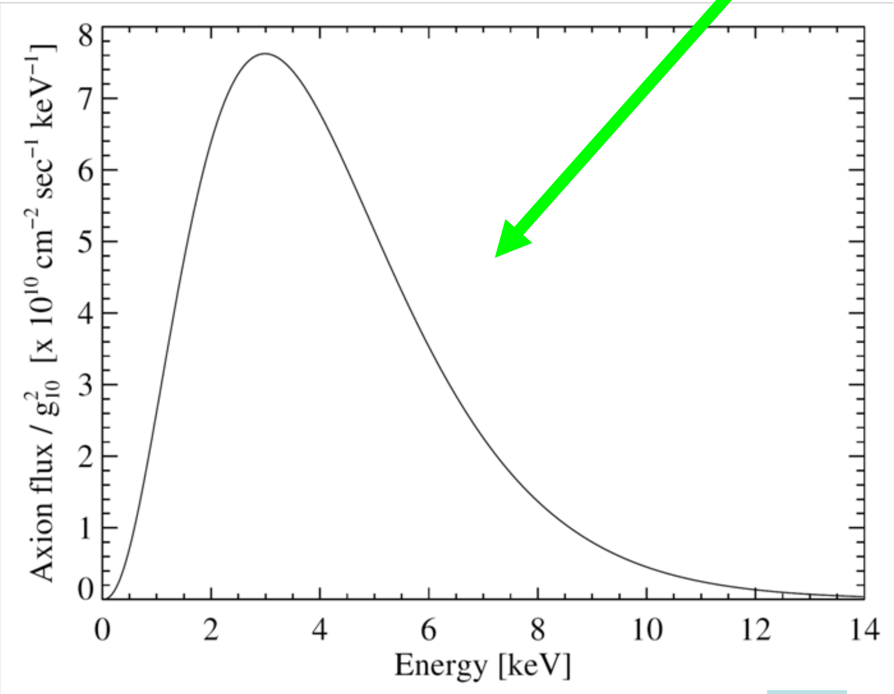

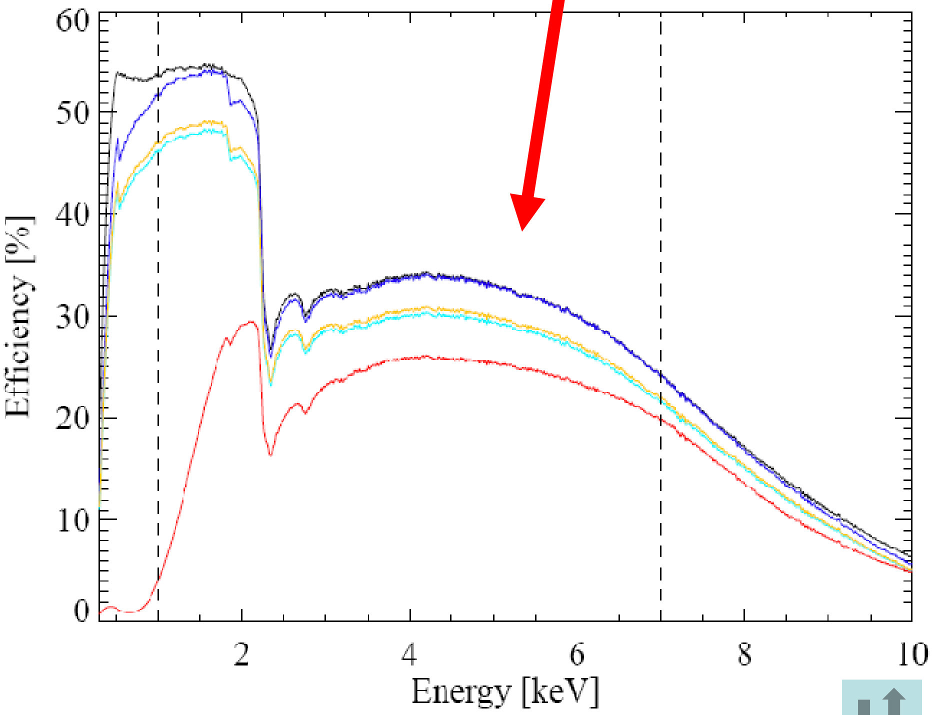

Exemplary Analysis of the ^{4}He data

Expected signal: Conversion probability

For one helium density setting P_k one expects $N_{\gamma,k}$ photons from axion-to-photon conversion via Primakoff-effect:

$$N_{\gamma,k} = N_\gamma(P_k, m_a, g_{a\gamma}^4) = \int \frac{d\Phi(E_a, g_{a\gamma}^2)}{dE_a} P_{a\to\gamma,k}(E_a, m_a, g_{a\gamma}^2)\,\varepsilon(E_a)\,\Delta t_k\,A\,dE_a$$

$$P_{a\to\gamma,k} = \left(\frac{Bg_{a\gamma}}{2}\right)^2 \frac{1}{q_k(E_a,m_a)^2 + \Gamma_k(E_a)^2/4}\left[1 + e^{-\Gamma_k(E_a)L} - 2e^{-\Gamma_k(E_a)L/2}\cos[q_k(E_a,m_a)L]\right]$$

$$P_{a\to\gamma,k} = \left(\frac{BLg_{a\gamma}}{2}\right)^2 \frac{\sin^2\left(q_k L/2\right)}{\left(q_k L/2\right)^2}$$

(for absorption $\Gamma = 0$)

Exemplary Analysis of the ^{4}He data

Expected signal: Conversion probability

$$P_{a\to\gamma,k}=\left(\frac{Bg_{a\gamma}}{2}\right)^2\frac{1}{q_k(E_a,m_a)^2+\Gamma_k(E_a)^2/4}\left[1+e^{-\Gamma_k(E_a)L}-2e^{-\Gamma_k(E_a)L/2}\cos[q_k(E_a,m_a)L]\right]$$

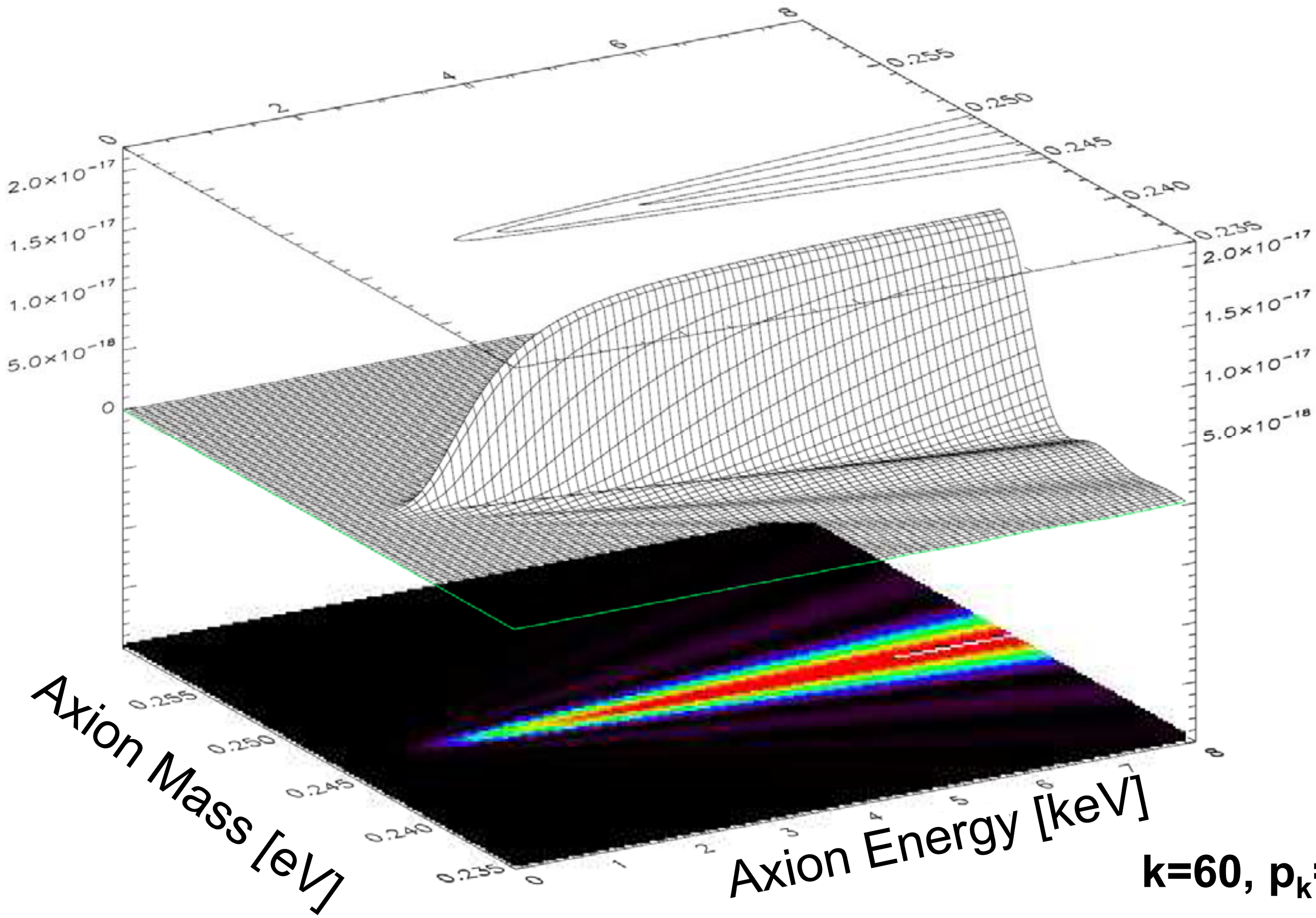

k=60, p_k=5.49 mbar

Exemplary Analysis of the ^{4}He data

Expected signal: Number of photons N_γ

$$N_{\gamma,k} = \int \frac{d\Phi(E_a, g_{a\gamma}^2)}{dE_a} P_{a\rightarrow\gamma,k}(E_a, m_a, g_{a\gamma}^2)\, \varepsilon(E_a)\, \Delta t_k\; A\, dE_a$$

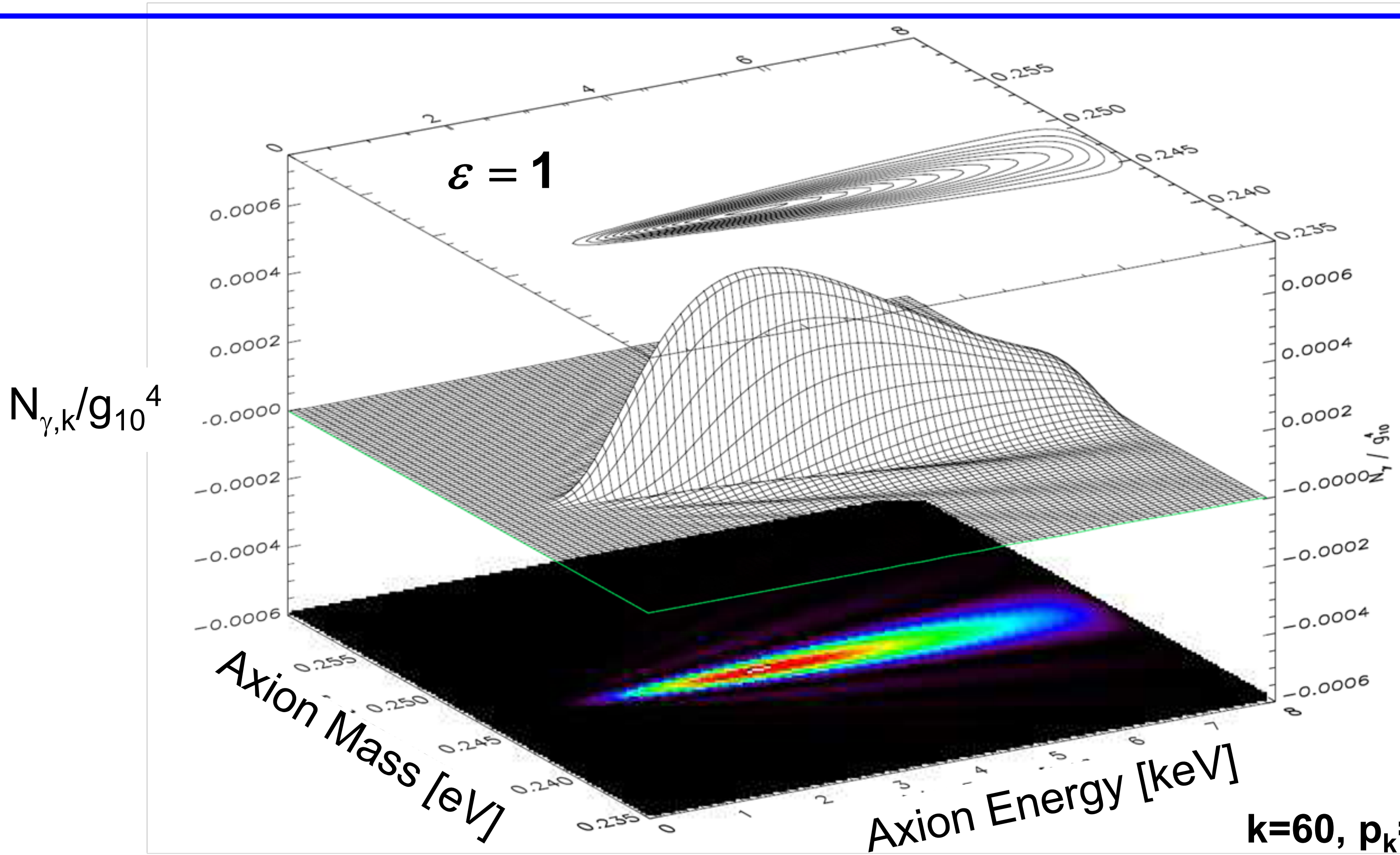

k=60, p_k=5.49 mbar

Exemplary Analysis of the ^{4}He data

Expected signal: Number of photons N_γ

$$N_{\gamma,k} = \int \frac{d\Phi(E_a, g^2_{a\gamma})}{dE_a} P_{a\to\gamma,k}(E_a, m_a, g^2_{a\gamma})\, \varepsilon(E_a)\, \Delta t_k\; A\, dE_a$$

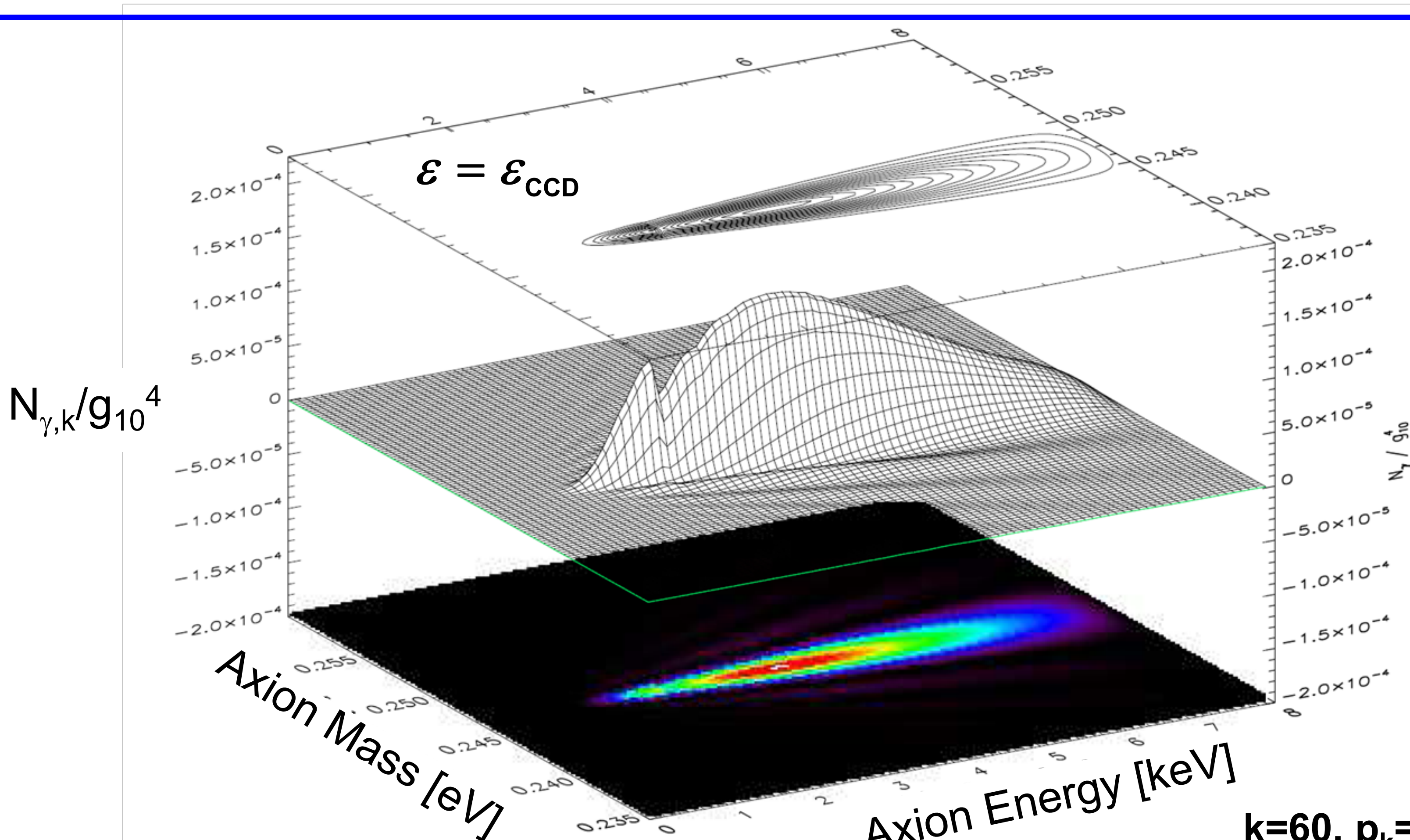

k=60, p_k=5.49 mbar

Exemplary Analysis of the ^{4}He data

Expected signal: Number of photons N_γ

$$N_{\gamma,k} = \int \frac{d\Phi(E_a, g_{a\gamma}^2)}{dE_a} P_{a\to\gamma,k}(E_a, m_a, g_{a\gamma}^2)\, \varepsilon(E_a)\, \Delta t_k\, A\, dE_a$$

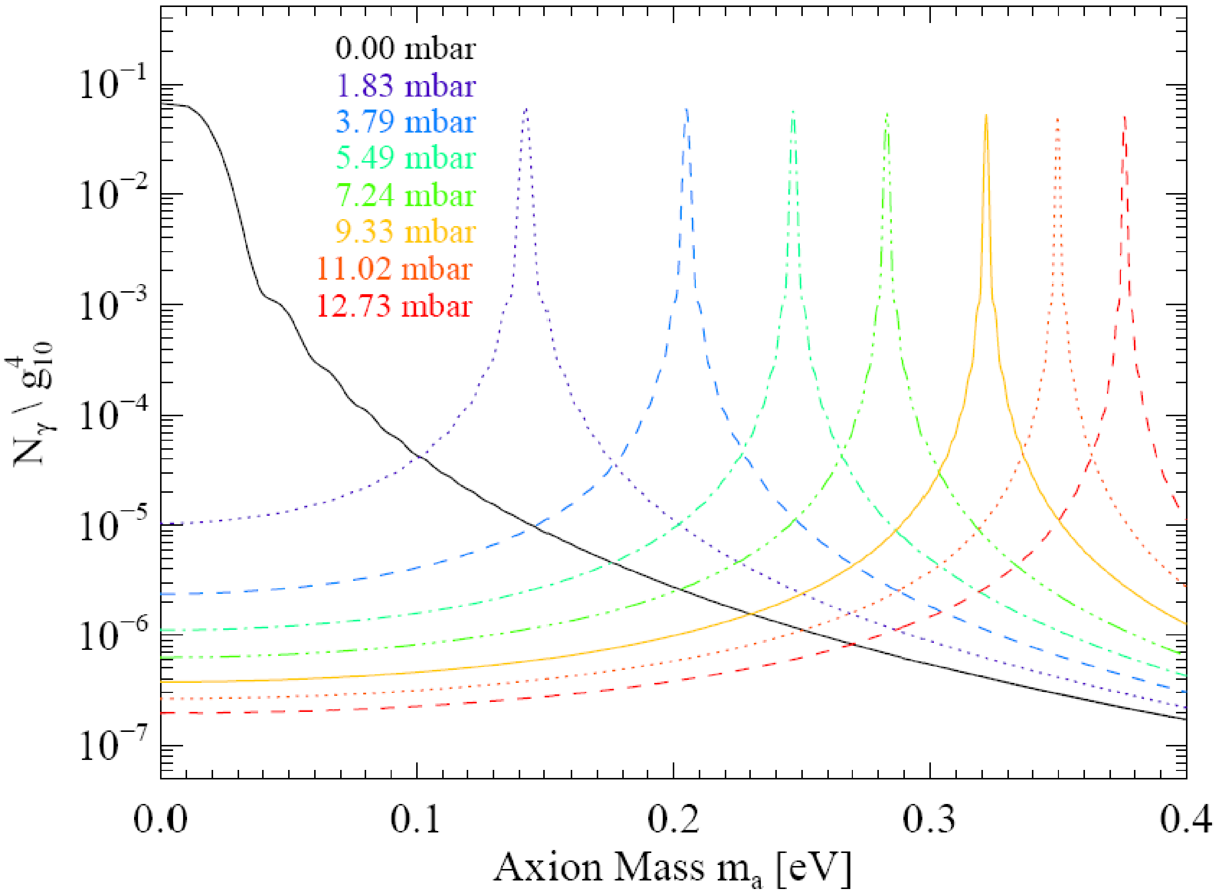

Exemplary Analysis of the ^{4}He data

Analysis: Definition of tracking and background

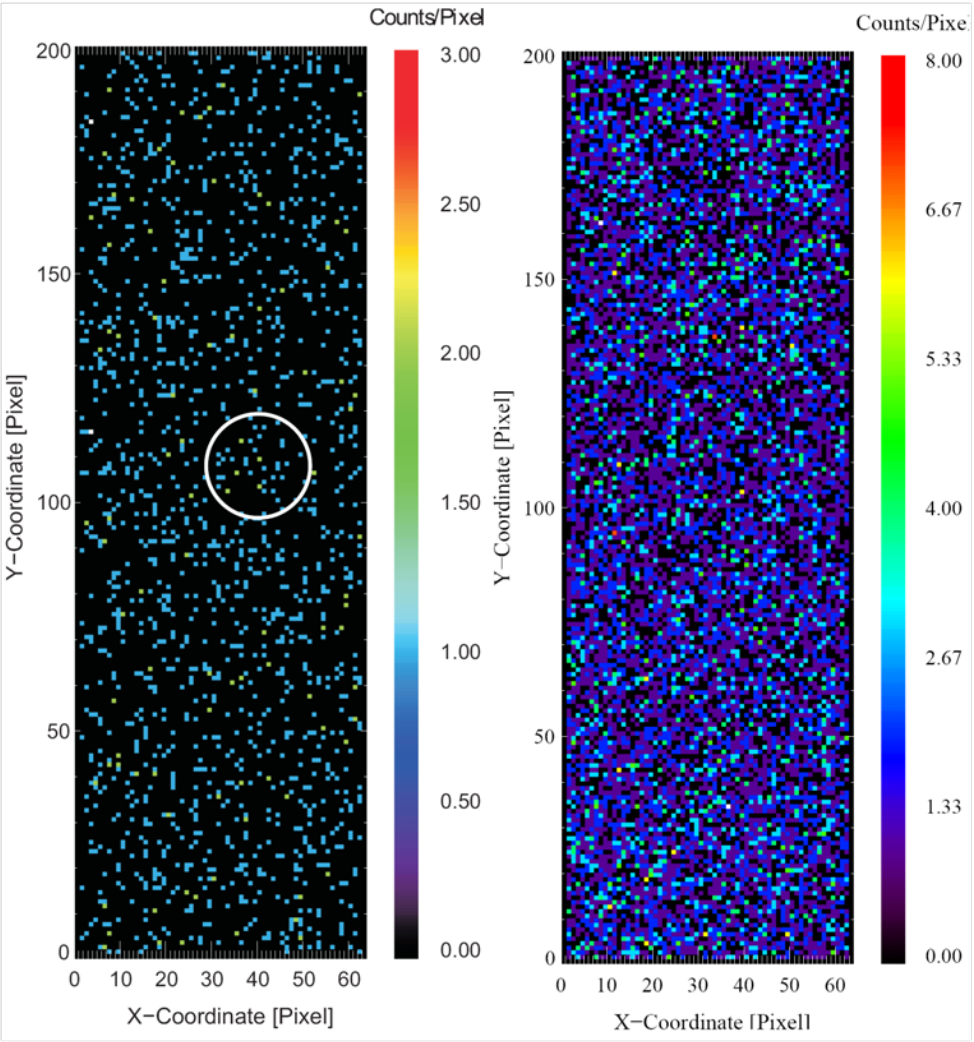

Tracking:

→ 294.8 h (1508/45 cts chip/spot)

→ 8.58 ± 0.17 x 10^{-5} cts/cm^2/s/keV

Background:

→ 2758.1 h (14245/430 cts chip/spot)

→ 8.66 ± 0.06 x 10^{-5} cts/cm^2/s/keV

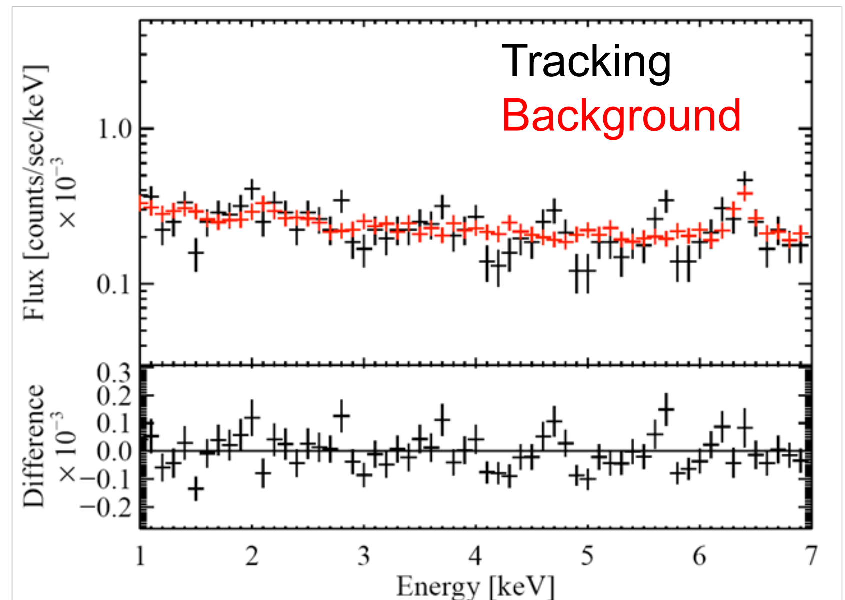

NO SIGNIFICANT AXION SIGNAL ABOVE BACKGROUND OBSERVED!

Exemplary Analysis of the ^{4}He data

Analysis: Maximum Likelihood Method

Expected counts in CCD for helium pressure P_k are Poissonian distributed with mean μ_{ik}

$$L_k = \prod_i^{20} e^{\mu_{ik}} \frac{\mu_{ik}^{n_{ik}}}{n_{ik}!} \Big/ \prod_i^{20} e^{n_{ik}} \frac{n_{ik}^{n_{ik}}}{n_{ik}!}$$

i	= Number of energy bin
k	= Number of pressure step
n_{ik}	= Total number of counts in tracking in energy bin i and pressure setting k
μ_{ik}	= b_{ik} + $(N_\gamma)_{ik}$ $(g_{a\gamma}{}^4, m_a)$
	= expected background + theoretical axion signal

Exemplary Analysis of the ^{4}He data

Analysis: Single pressure settings

Expected counts in CCD for helium pressure P_k are Poissonian distributed with mean μ_{ik}

$$L_k = \prod_i^{20} e^{\mu_{ik}} \frac{\mu_{ik}^{n_{ik}}}{n_{ik}!} \Bigg/ \prod_i^{20} e^{n_{ik}} \frac{n_{ik}^{n_{ik}}}{n_{ik}!}$$

i = Number of energy bin
k = Number of pressure step
n_{ik} = Total number of counts in tracking in energy bin i and pressure setting k
μ_{ik} = b_{ik} + $(N_\gamma)_{ik}$ $(g_{a\gamma}{}^4, m_a)$
= expected background + theoretical axion signal

- **Single pressure settings**
  → Calculation of single pressure likelihood functions L_k
  → χ^2-Distribution $\chi_k{}^2 = -2 \ln L_k$
  → Upper limit via integration of Bayesian probability up to 95%
  → **Exclusion plot for single pressure settings**

Exemplary Analysis of the ^4He data

Analysis: Single pressure settings

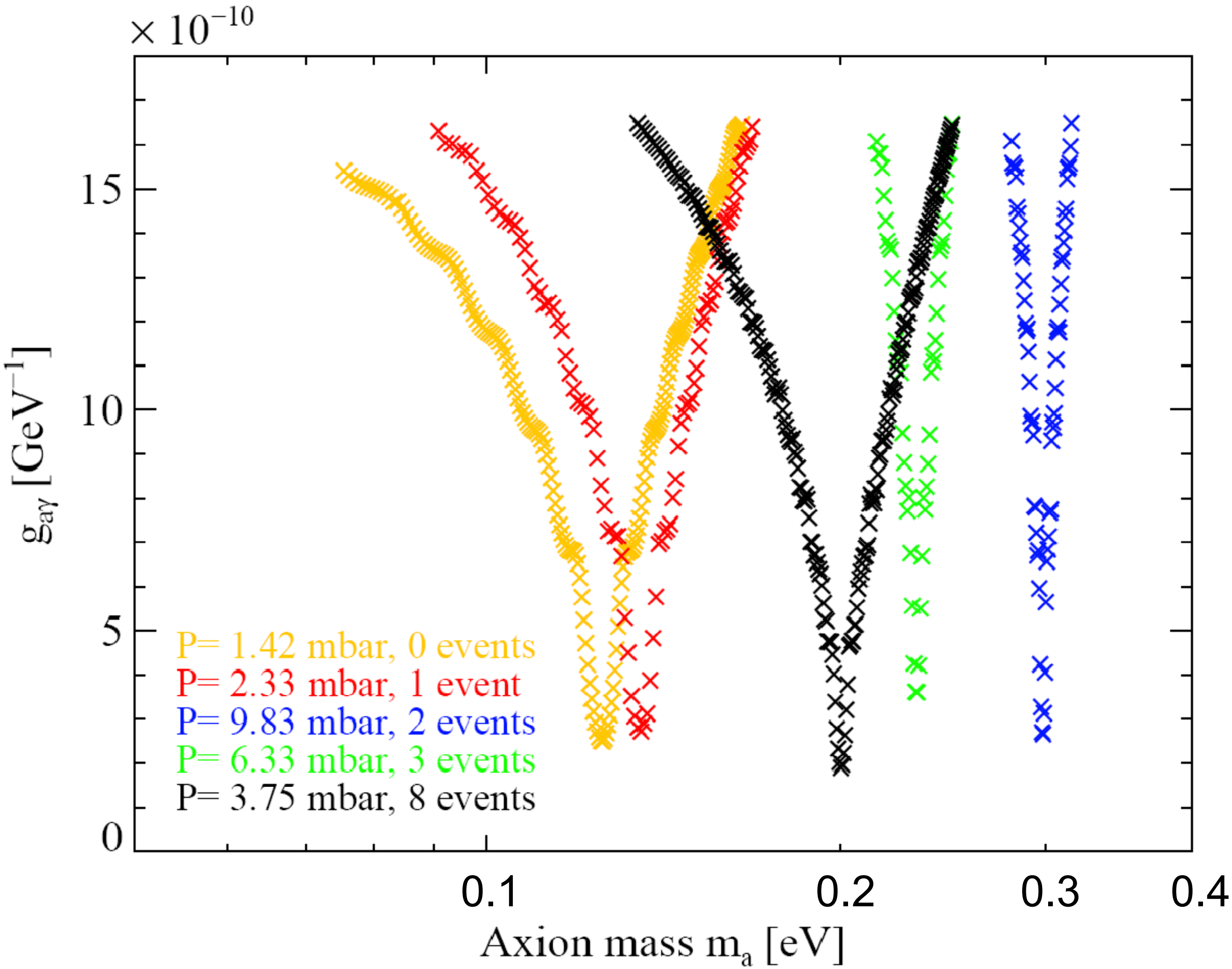

Exemplary Analysis of the ^4He data

Analysis: All pressure settings

Expected counts in CCD for helium pressure P_k are Poissonian distributed with mean μ_{ik}

$$L_k = \prod_i^{20} e^{\mu_{ik}} \frac{\mu_{ik}^{n_{ik}}}{n_{ik}!} \Bigg/ \prod_i^{20} e^{n_{ik}} \frac{n_{ik}^{n_{ik}}}{n_{ik}!}$$

i = Number of energy bin

k = Number of pressure step

n_{ik} = Total number of counts in tracking in energy bin i and pressure setting k

μ_{ik} = b_{ik} + $(N_\gamma)_{ik}$ $(g_{a\gamma}{}^4, m_a)$
= expected background + theoretical axion signal

Analysis: All pressure settings

Expected counts in CCD for helium pressure P_k are Poissonian distributed with mean μ_{ik}

$$L_k = \prod_i^{20} e^{\mu_{ik}} \frac{\mu_{ik}^{n_{ik}}}{n_{ik}!} \Bigg/ \prod_i^{20} e^{n_{ik}} \frac{n_{ik}^{n_{ik}}}{n_{ik}!}$$

i = Number of energy bin

k = Number of pressure step

n_{ik} = Total number of counts in tracking in energy bin i and pressure setting k

μ_{ik} = b_{ik} + $(N_\gamma)_{ik}$ $(g_{a\gamma}{}^4, m_a)$
= expected background + theoretical axion signal

- **Combination of all pressure settings**
  - → Determination of the global likelihood function L via multiplication of likelihoods for all pressure settings $L = \Pi L_k$
  - → Global χ^2-Distribution $\chi^2 = -2 \ln L$
  - → Upper limit via integration of Bayesian probability up to 95%
  - → **Exclusion plot for all pressure settings**

Exemplary Analysis of the ^4He data

CCD result for Phase II with ^4He

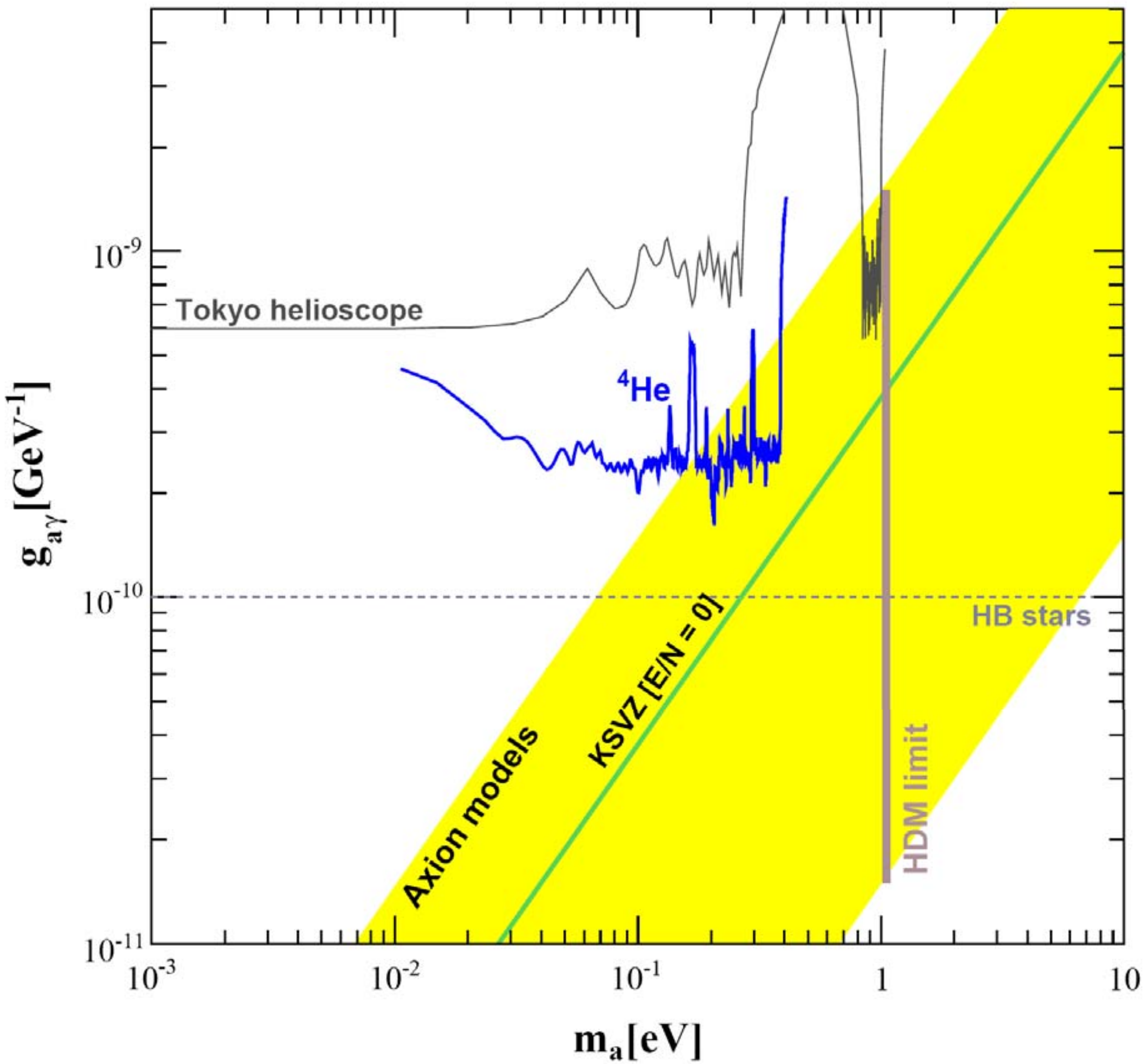

Exemplary Analysis of the ^{4}He data

Combined CCD result for Phase I and Phase II with ^{4}He

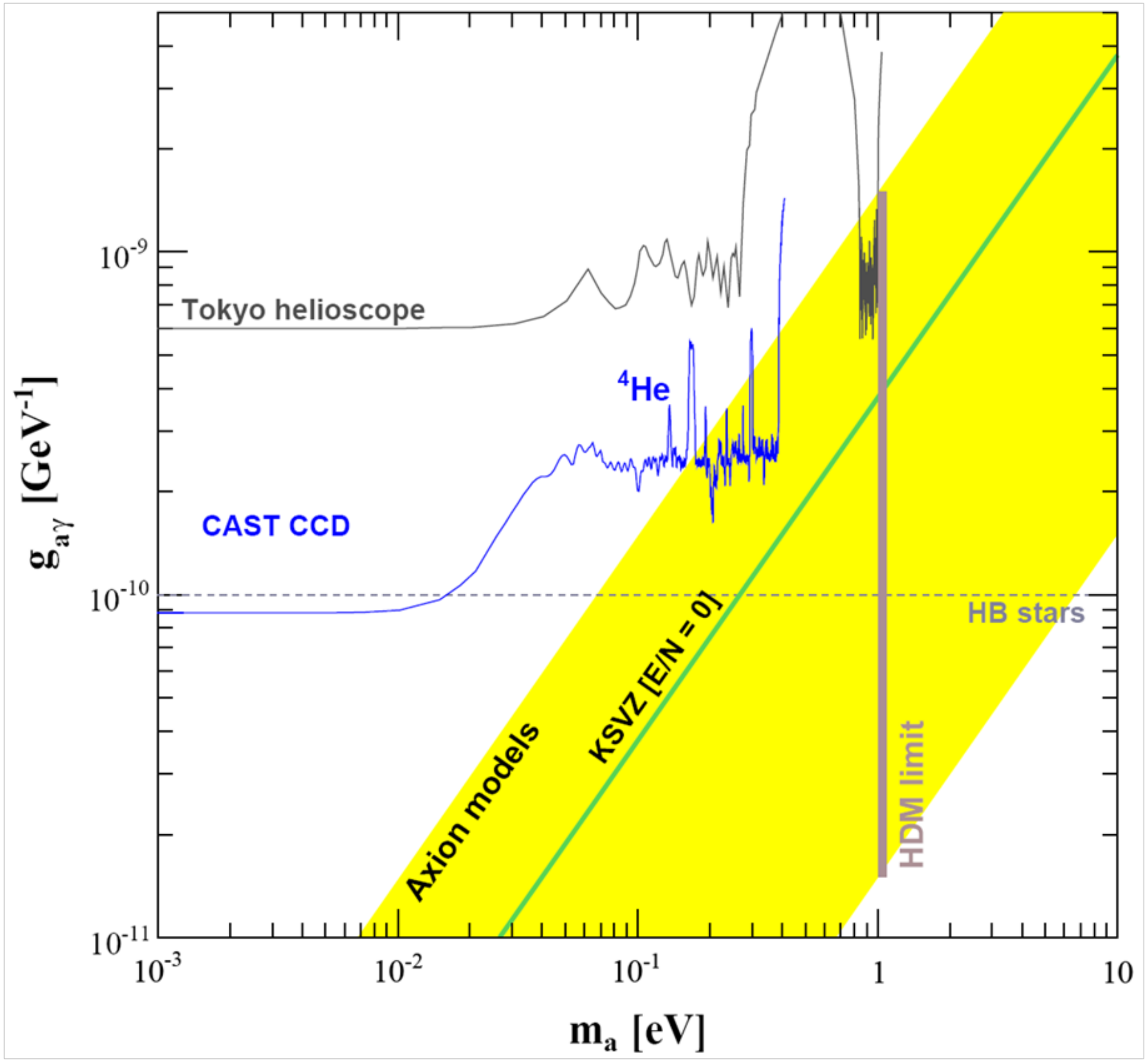

Results and Prospects

CAST Result Phase I

- No significant signal over background
- CAST Phase I yielded most restrictive experimental upper limit in wide axion mass range
- CAST is more sensitive than best astrophysical limit for axion masses $m_a < 0{,}02$ eV
- Improvement of the upper limit compared to previous experiments by factor of 7

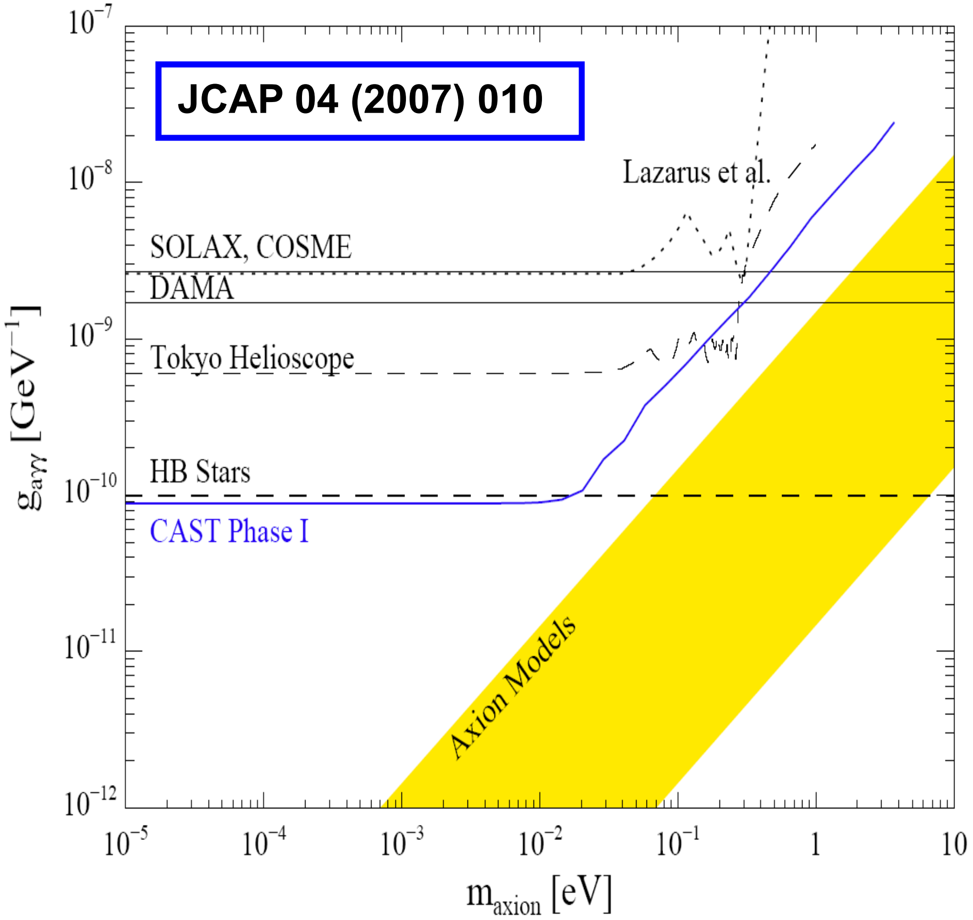

Upper Limit $g_{a\gamma\gamma}$ for $m_a < 0{,}02$ eV

$g_{a\gamma}$ (95%) = $0{,}88 \times 10^{-10}$ GeV^{-1}

CAST Result Phase I and II with ^4He

- 160 measured p-settings with ^4He in the magnet (p=13.4 mbar, m_a=0.39 eV)
- No significant signal observed
- CAST enters in theoretically favored model regions
- Typical upper limit:

  $g_{a\gamma}$ (95%) = 2,2 x 10^{-10} GeV^{-1}

  for m_a < 0.39 eV
- ^4He analysis completed

  → JCAP 02 (2009) 008
- **^3He measurements ongoing!**

  (Over 480 new ^3He steps done!)

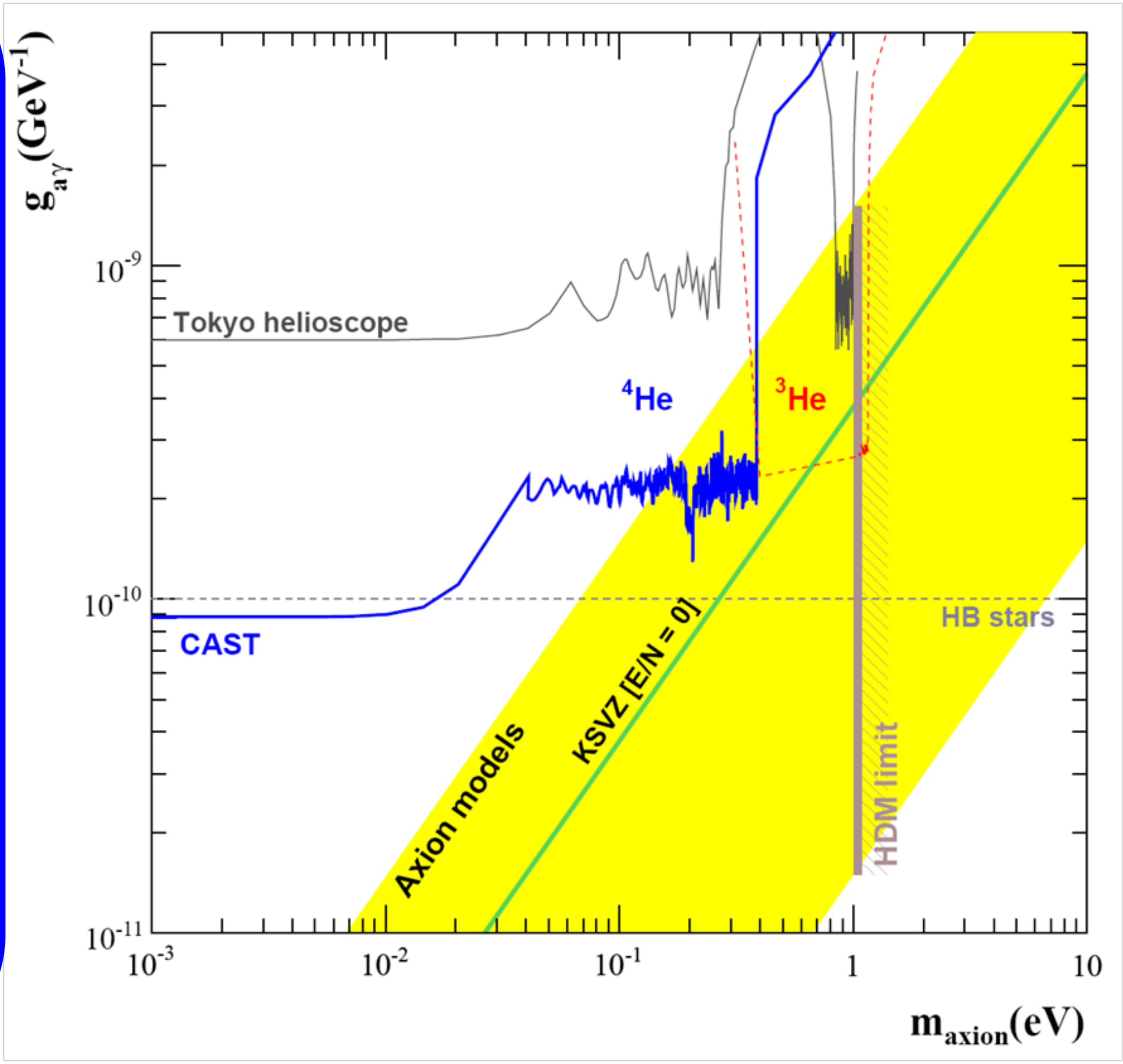

Additional Searches at CAST: HE and 14.4 keV Axions

„Search for solar axion emission from ^{7}Li and D(p,γ)^{3}He nuclear decays with the CAST γ-ray calorimeter"

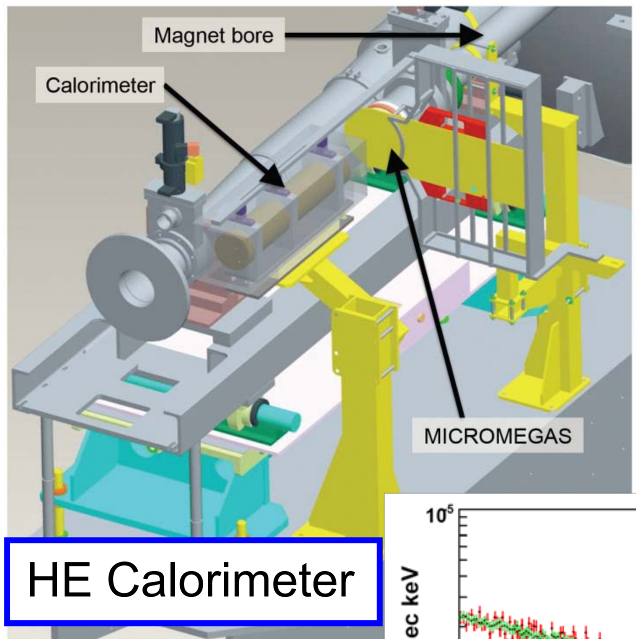

HE Calorimeter

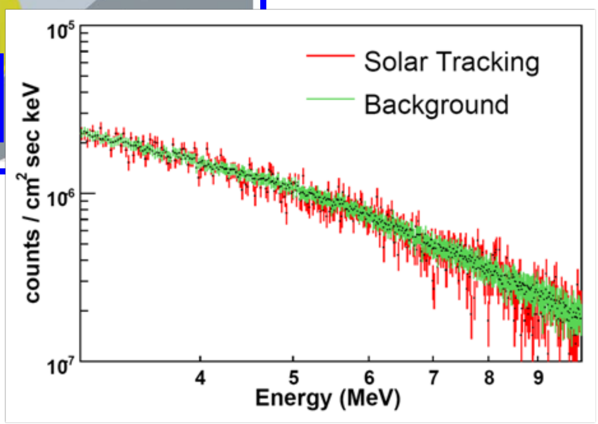

arXiv:0904.2103

Results and Prospects

Additional Searches at CAST: HE and 14.4 keV Axions

„Search for solar axion emission from ^{7}Li and D(p,γ)^{3}He nuclear decays with the CAST γ-ray calorimeter“

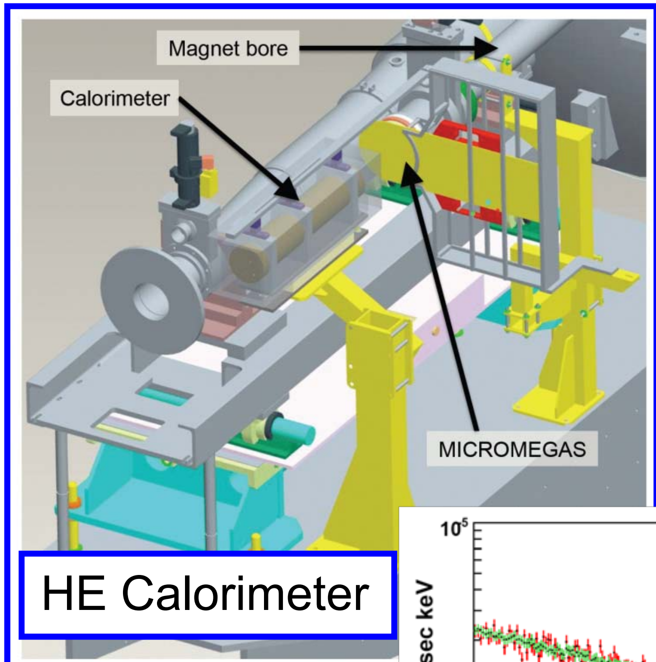

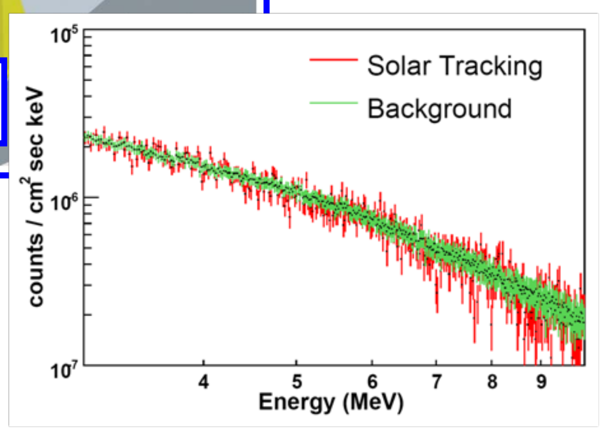

arXiv:0904.2103

„Search for 14.4 keV solar axion emitted in the M1-transition of ^{57}Fe nuclei with CAST“

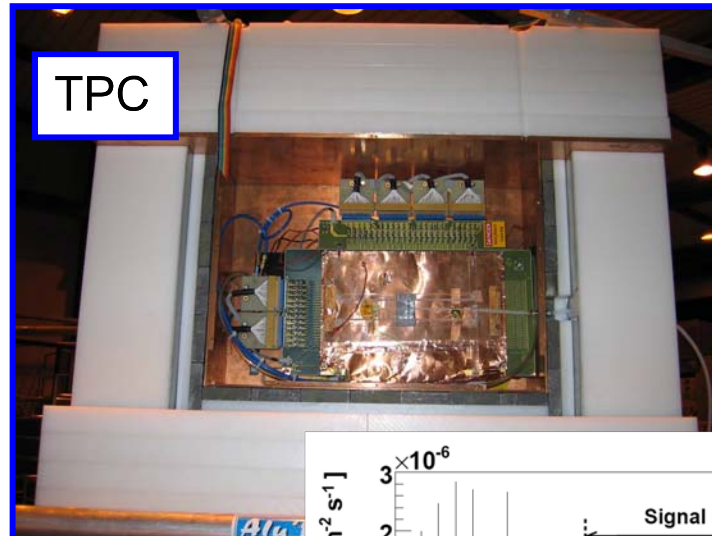

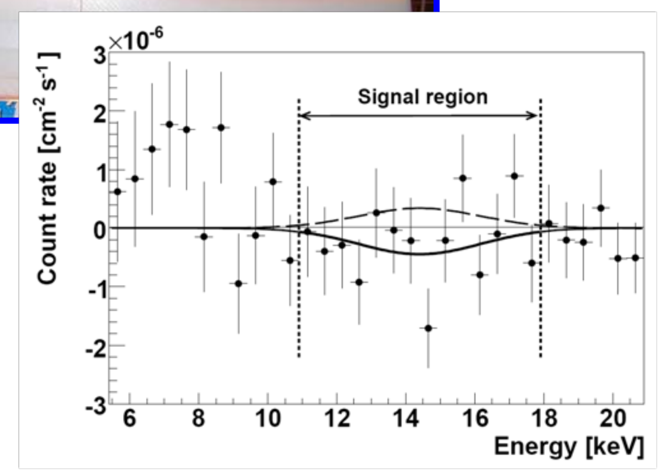

arXiv:0906.4488

Additional Searches at CAST: LES Axions and Galactic Sources

„Search for low energy solar axion with CAST“

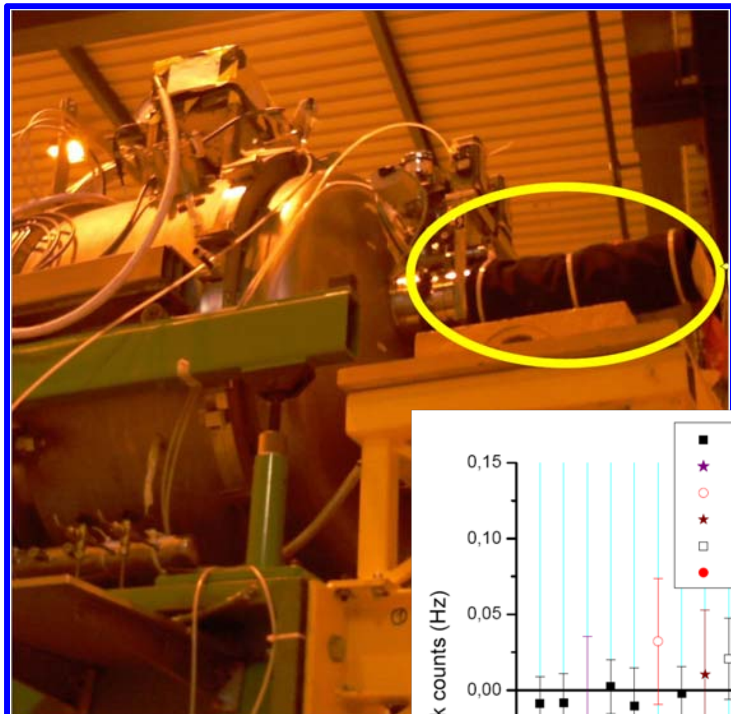

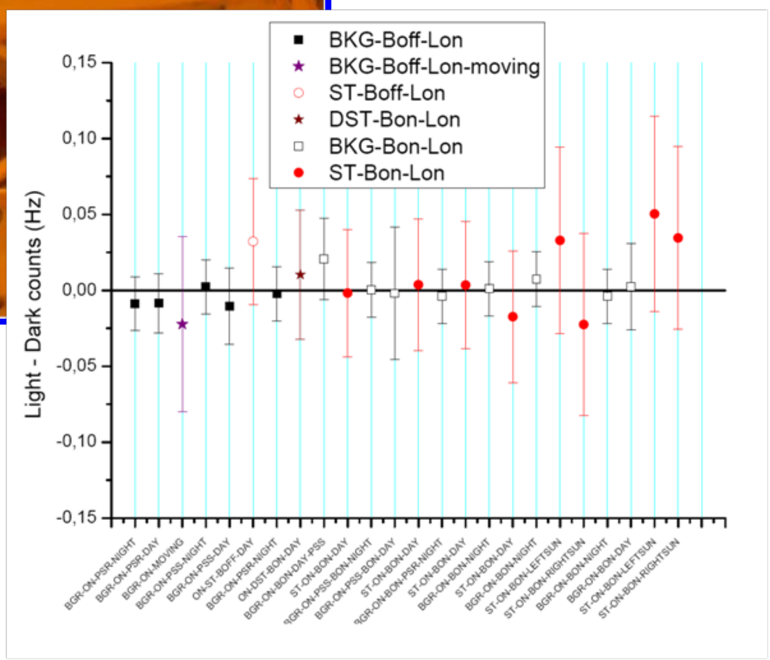

arXiv:0809.4581

See also contributions to 5th Patras Workshop on Axions, WIMPs and WISPs

→ http://axion-wimp.desy.de/

Additional Searches at CAST: LES Axions and Galactic Sources

„Search for low energy solar axion with CAST“

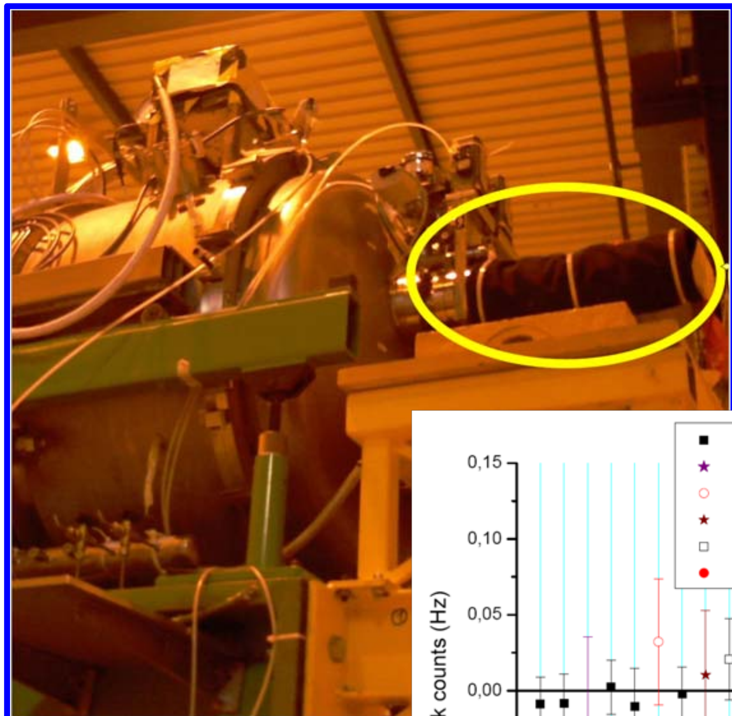

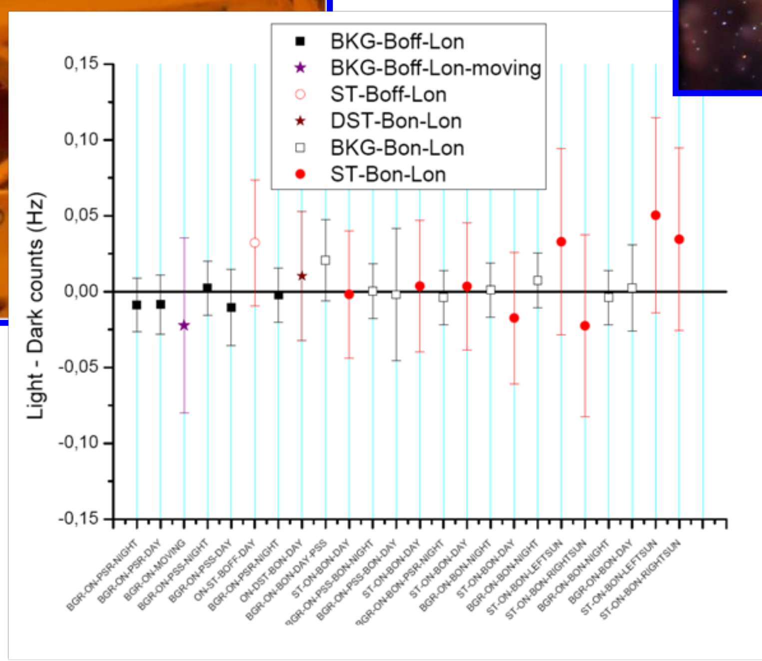

arXiv:0809.4581

Search for Axions from galactic sources at CAST/ Sky Survey

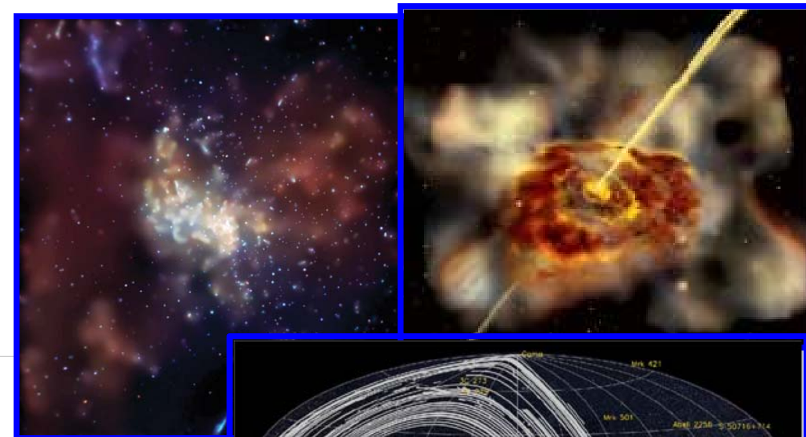

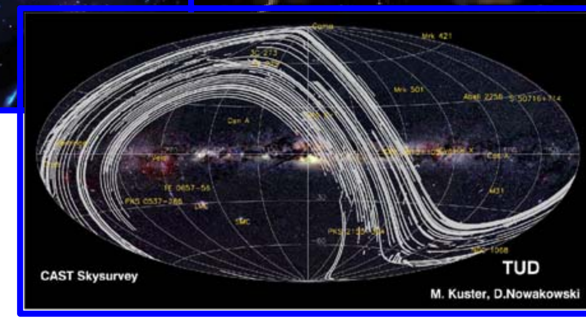

See also contributions to 5th Patras Workshop on Axions, WIMPs and WISPs

→ http://axion-wimp.desy.de/

Results and Prospects

Towards future axion helioscope searches

- Along the years CAST gained valuable expertise in working with the helioscope technique
- Possible improvements for next generation helioscopes:
  - → New low background detectors
  - → X-ray focussing devices
  - → More flexible movement
  - → More powerful magnet !!!
- See also talk of T. Papaevangelou in the recent workshop *„New opportunities in the Physics Landscape at CERN“*

Magnet

Stronger field, bigger cross sectional area,...

$$g_{a\gamma} \propto (B\,L)^{-1/2}\,(A)^{-1/4}\,(b^{1/8}/t^{1/8})$$

Detectors

Very low background and/or X-ray telescopes

Movement System

Extension of Observation time

Towards future axion helioscope searches

Large parts of the model region for QCD axions could be Studied in the coming decade

→ Combination of Helioscopes experiments and Dark matter axion searches such as ADMX

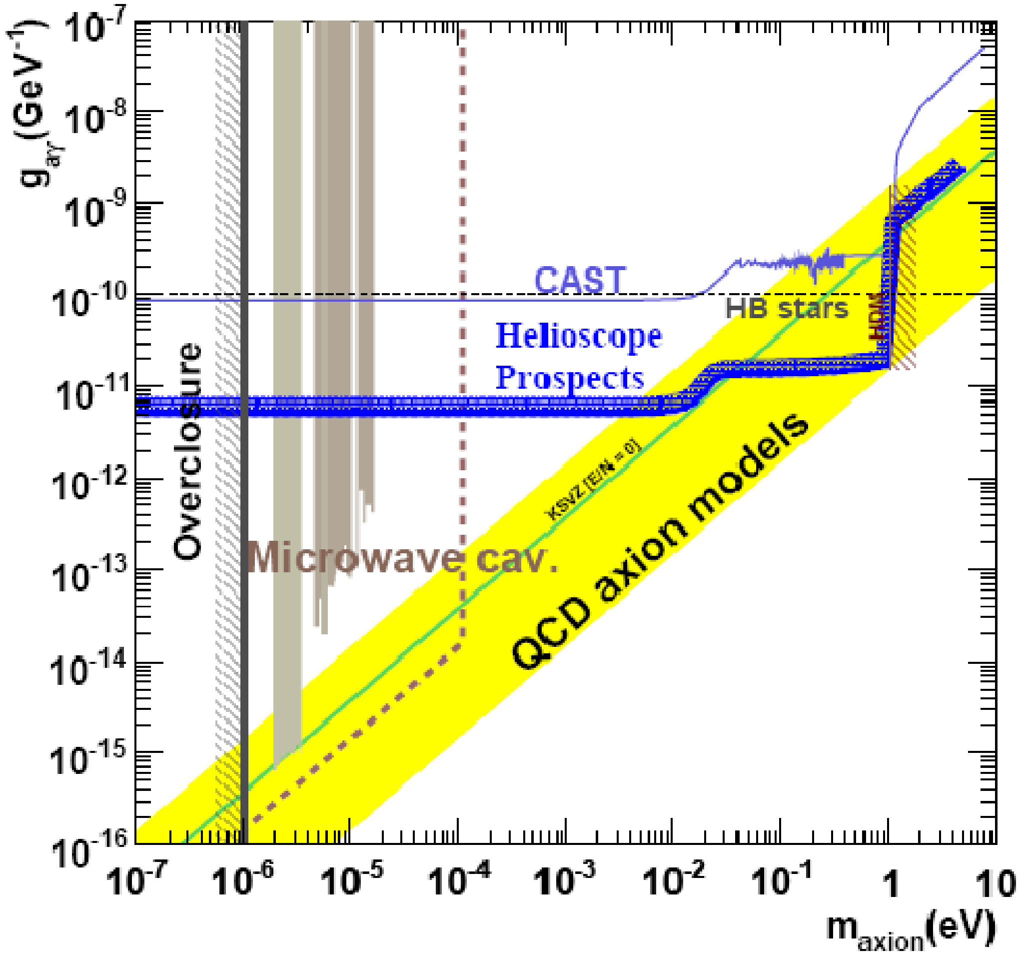

Latest Results of Phase I and II

CAST Phase I

→ No significant axion signal observed
→ Best experimental upper limit in large axion mass range up to 0.02 eV

$$g_{a\gamma}\ (95\%) = 0.88 \times 10^{-10}\ \mathrm{GeV}^{-1}$$

→ Comparable to best astrophysical limit

CAST Phase II

→ Upgraded detectors and sophisticated gas system for the use of helium
→ CAST enters theoretically favored axion parameter space
→ ^{4}He run completed with typical upper limit for $0.02 < m_a < 0.39$ eV of

$$g_{a\gamma}\ (95\%) = 2.2 \times 10^{-10}\ \mathrm{GeV}^{-1}$$

→ Data taking with ^{3}He since 2007 (approved till 2010): $m_a < 1.2$ eV [0.89 eV]

More interesting Physics done/to be done at CAST

→ High energy axions / 14.4 keV axions
→ Low energy solar axions (LES axions)
→ Galactic tracking for non-solar axions / Sky Survey

Axions ?!? Not yet... but stay tuned...

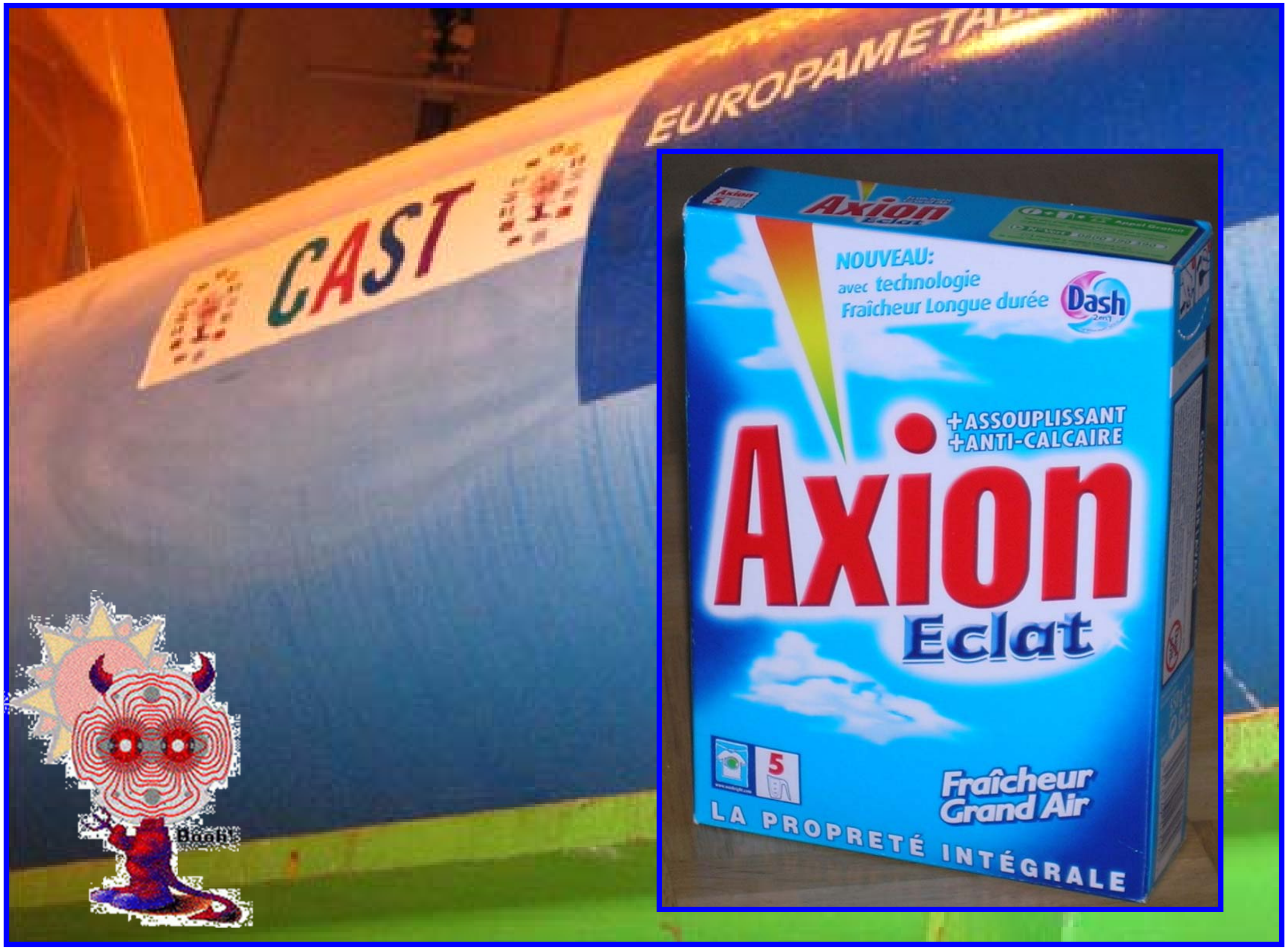

Thank you!

Backup

Backup: Theoretical Motivation for Axions

The strong CP-problem

- New term in Lagrangian violates both P and CP:

$$G^a_{\mu\nu}\tilde{G}^{\mu\nu}_a \propto \vec{\mathbf{E}}\cdot\vec{\mathbf{B}}$$

- Compare to

$$G^a_{\mu\nu}G^{\mu\nu}_a \propto \vec{\mathbf{B}}^2 - \vec{\mathbf{E}}^2$$

Since:

$$P(\vec{\mathbf{E}}) = -\vec{\mathbf{E}},\ \ P(\vec{\mathbf{B}}) = +\vec{\mathbf{B}}$$

$$C(\vec{\mathbf{E}}) = -\vec{\mathbf{E}},\ \ C(\vec{\mathbf{B}}) = -\vec{\mathbf{B}}$$

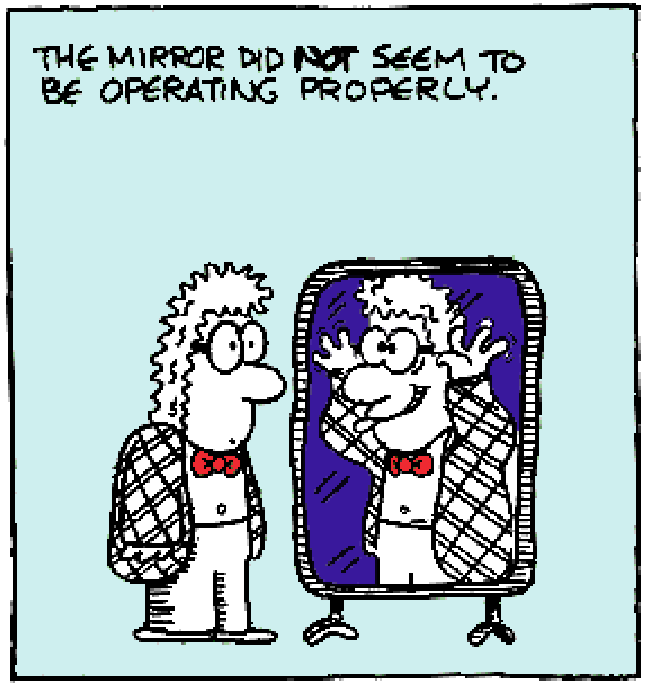

- **Strong CP-Problem:**

No violation of CP in strong interactions observed so far!

Could be observed via:

Electric dipole moment (EDM) of the neutron (Dependency on θ)

Backup: X-ray mirror optics and CCD detector

Experimental Setup

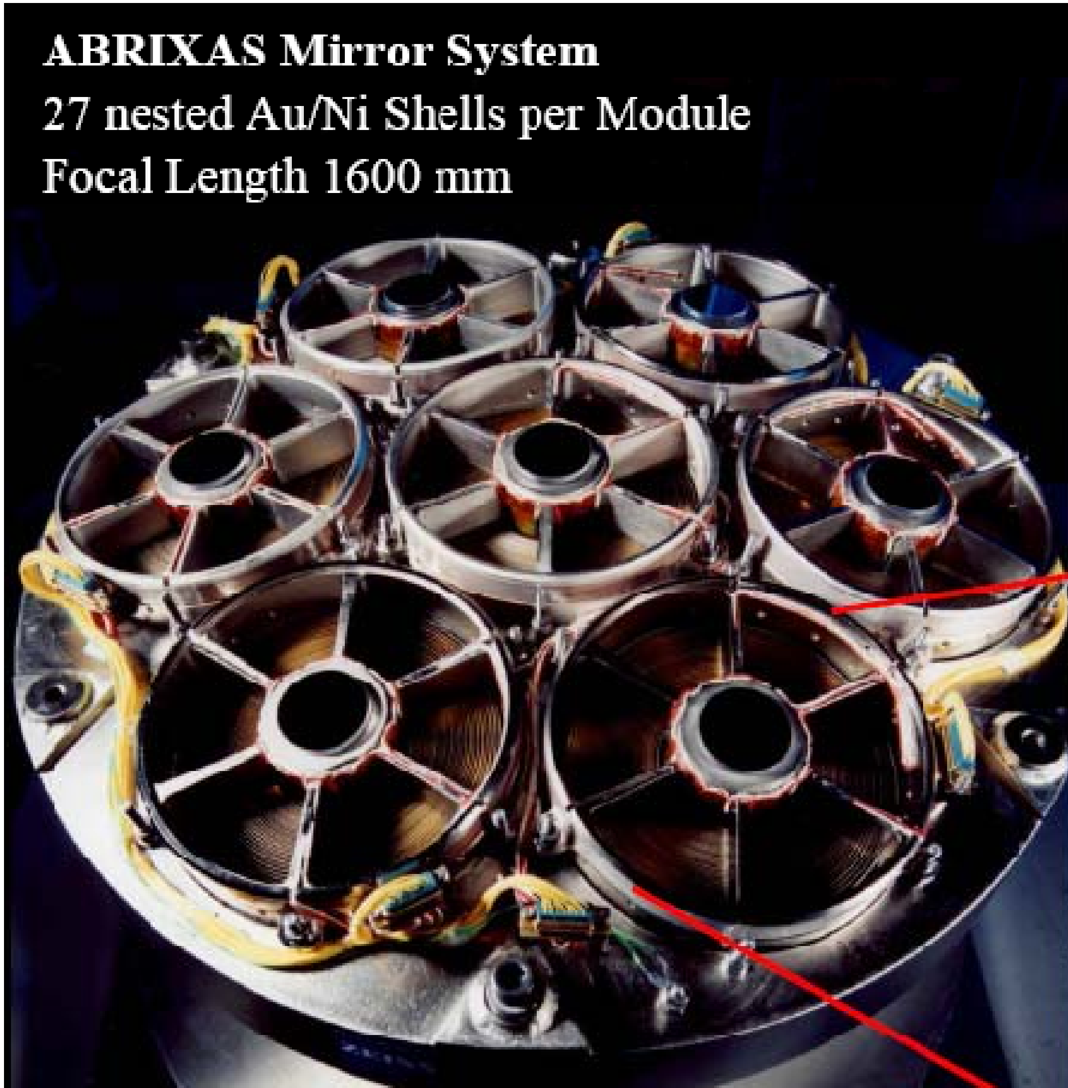

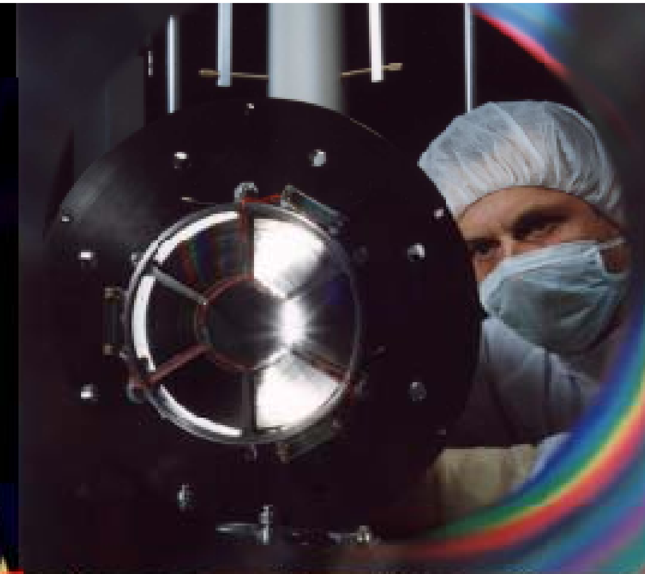

CAST Setup

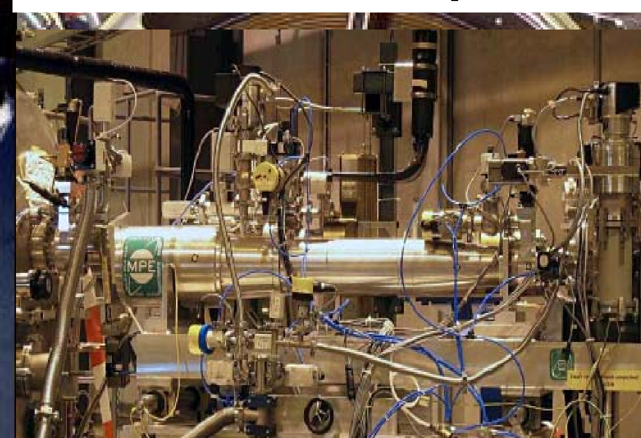

Backup: X-ray mirror optics and CCD detector

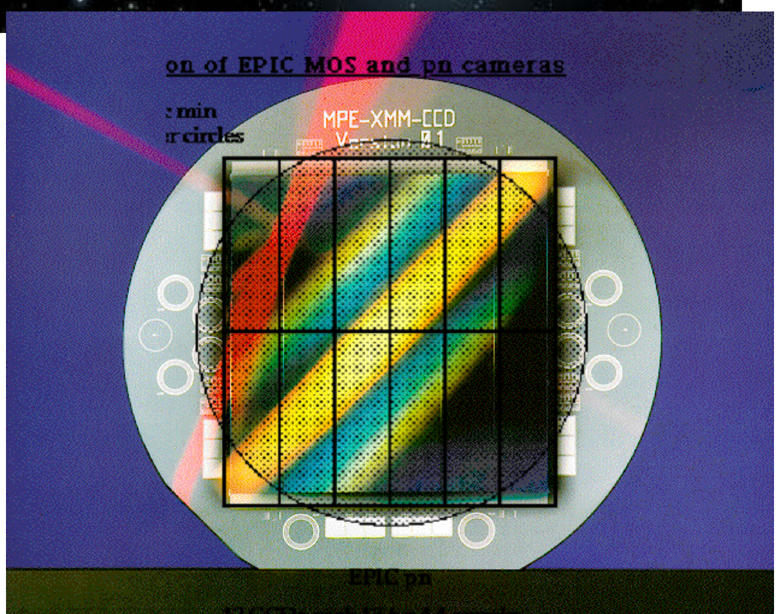

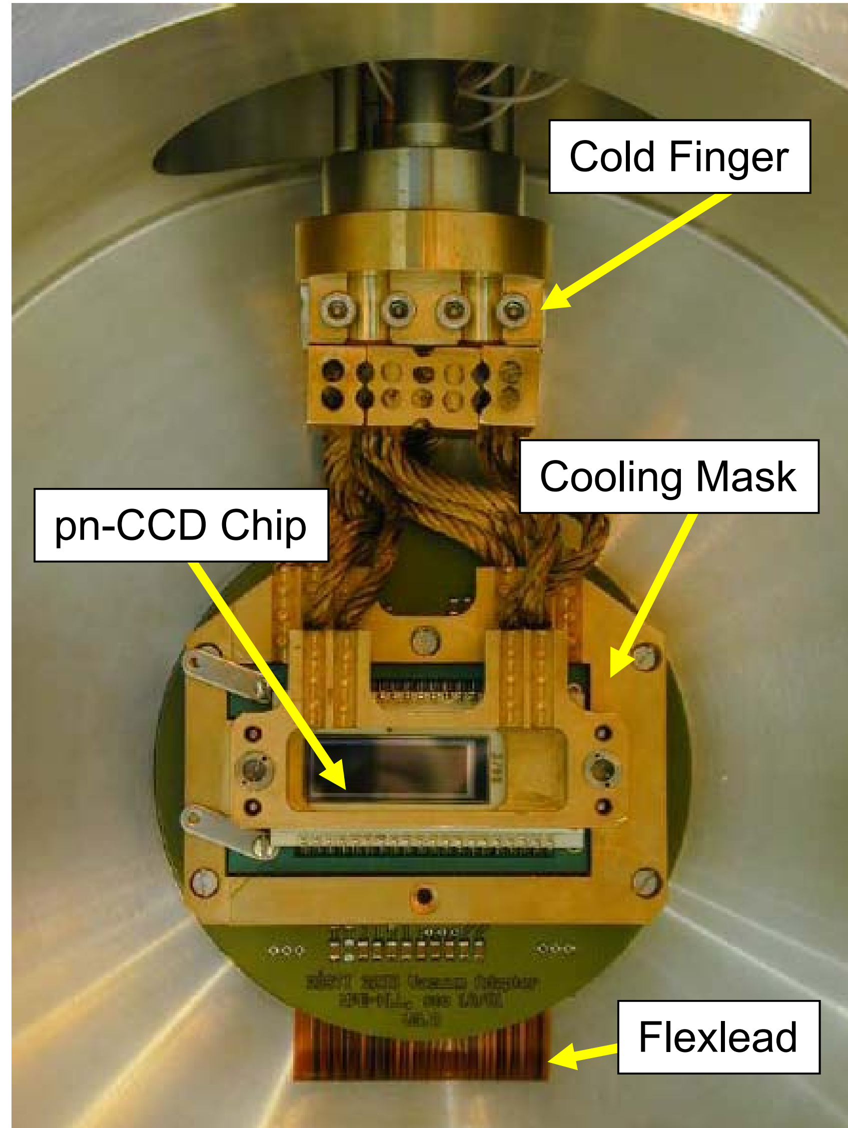

Backup: X-ray mirror optics and CCD detector

Working principle of the CCD detector

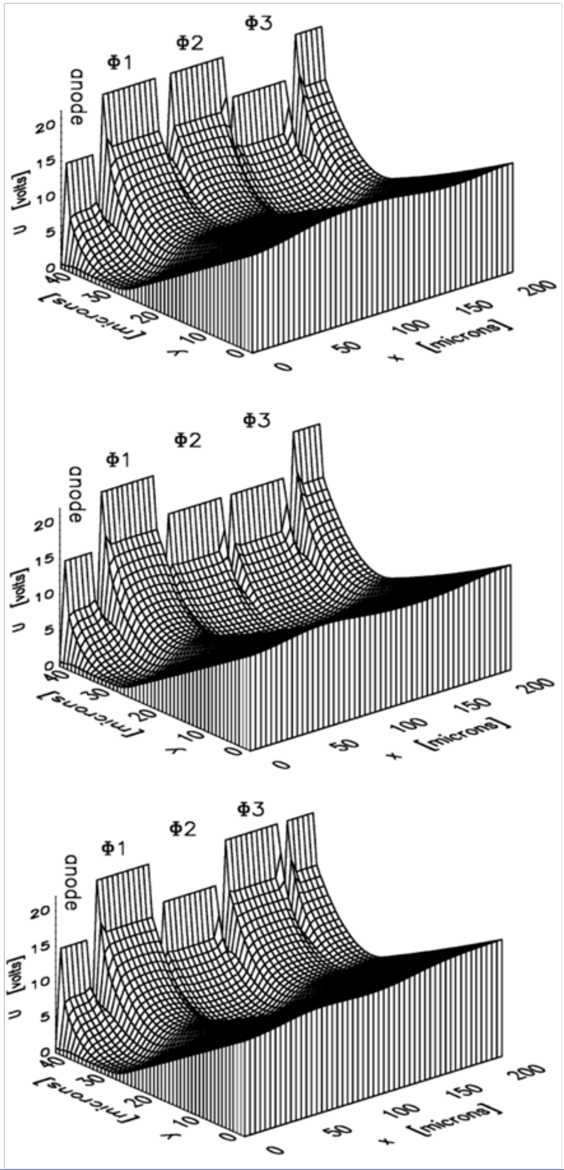

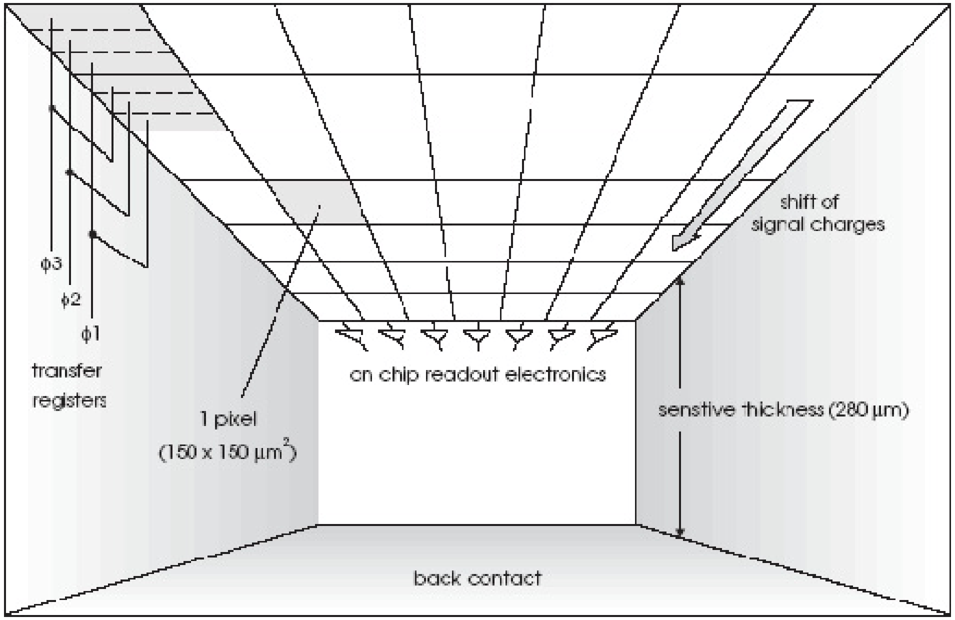

X-ray mirror optics and CCD detector

In-situ calibration of detector

Daily calibration with ^{55}Fe before run

Energy resolution: 170 eV @ 5.9 keV

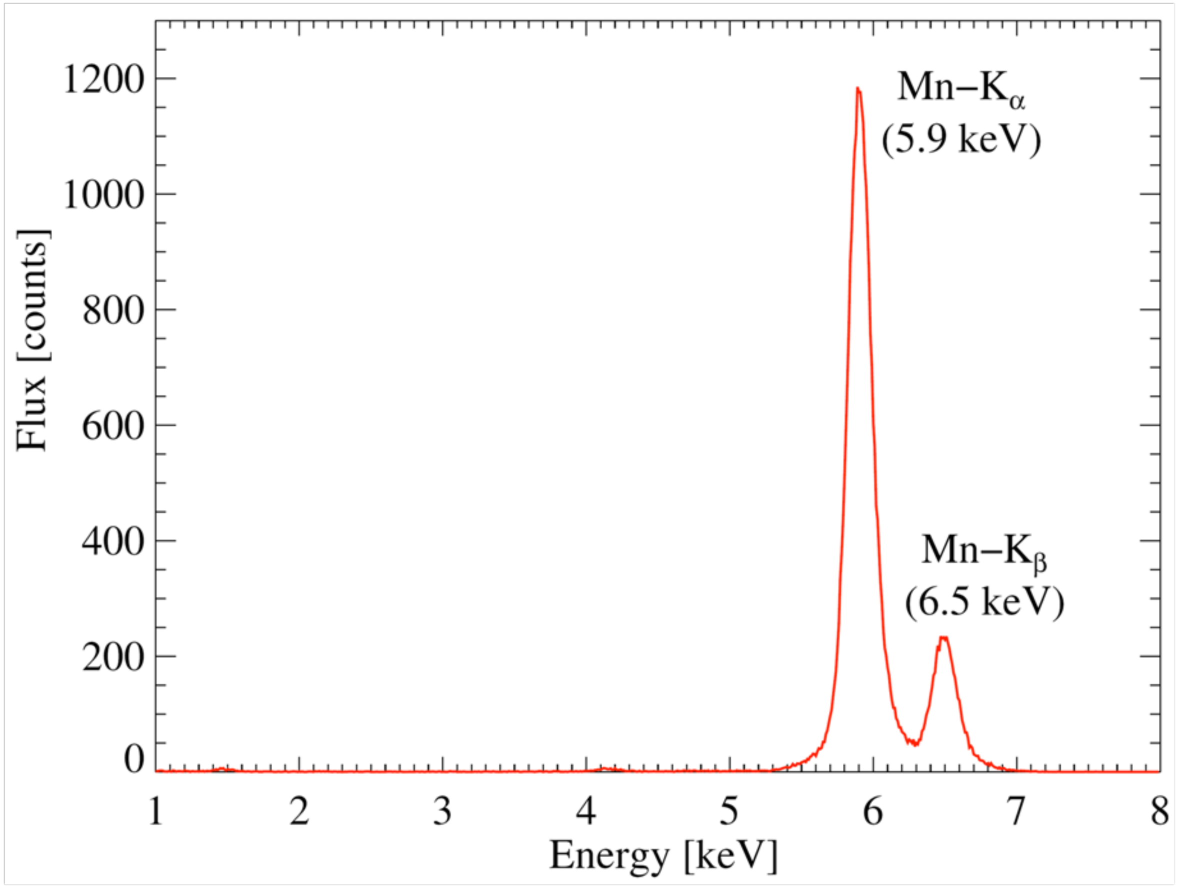

Analysis of CCD data for the ^{4}He Phase

Analysis: Absence of a signal